Influence of pre-Andean history over Cenozoic foreland deformation: Structural styles in the Malargüe fold-and-thrust belt at 35°S, Andes of Argentina

José F. Mescua[1,2], Laura B. Giambiagi[1,2], Andrés Tassara[3], Mario Gimenez[2,4], and Víctor A. Ramos[2,5]

[1]*IANIGLA (Instituto Argentino de Nivología, Glaciología y Ciencias Ambientales), Centro Científico Tecnológico Mendoza, Av. Ruiz Leal s/n, Parque General San Martín, Mendoza, 5500, AP 330, Argentina*

[2]*CONICET (Consejo Nacional de Investigaciones Científicas y Técnicas), Av. Rivadavia 1917, Ciudad Autónoma de Buenos Aires, C1033AAJ, Argentina*

[3]*Departamento de Ciencias de la Tierra, Universidad de Concepción, Victor Lamas 1290, Barrio Universitario, Concepción, Casilla 160-C, Chile*

[4]*Instituto Geofísico Sismológico Volponi, Facultad de Ciencias Exactas, Físicas y Naturales, Universidad Nacional de San Juan, Av. Ignacio de la Roza y Meglioli, Rivadavia, 5400 San Juan, Argentina*

[5]*Laboratorio de Tectónica Andina del Instituto de Estudios Andinos, Universidad de Buenos Aires, Ciudad Universitaria, Pabellón II, Intendente Güiraldes 2160, Ciudad Autónoma de Buenos Aires, C1428EHA, Argentina*

ABSTRACT

The Andes are the classic example of a subduction-related orogen. Segmentation of the orogenic belt is related to dynamics of the subduction zone and to upper plate thermomechanical properties. Understanding the controlling factors on deformation along the orogen requires studying cross sections at different latitudes and determining the respective roles of plate interactions, upper plate weakness zones, and crustal architecture. A newly constructed balanced cross section of the Argentinean Andes at 35°S, in the transition between a flat-slab and a normal subduction segment, shows tectonic inversion of Mesozoic normal faults and development of new thrusts during Andean shortening. Estimated shortening of 26.2 km, equivalent to 22% of the initial length, is lower than previous estimates obtained from partial cross sections using non-inversion structural models. Comparison of this estimate with crustal area balance constrained by geophysical data indicates that (1) crustal thickness was varied across the transect before Andean shortening, with a thick (~45 km) crustal block to the west related to late Paleozoic orogeny, and a thinner block (~32 km) in the east related to Mesozoic stretching; and (2) a structural model incorporating tectonic inversion is consistent with regional shortening and crustal thickness trends. Our results underscore the role of the inherited characteristics of the upper plate in subduction-related orogens, including preexisting faults and preorogenic crustal thickness variations.

INTRODUCTION

The eastern flank of the Andean orogen is characterized by the development of foreland fold-and-thrust belts with a segmentation defined by variations in structural style and shortening amounts (Kley et al., 1999). As noted by many (e.g., Gansser, 1973; Barazangi and Isacks, 1976; Jordan et al., 1983; Allmendinger et al., 1983; Isacks, 1988; Allmendinger and Gubbels, 1996; Ramos, 1999; Kley et al., 1999), the segmentation of the foreland fold-and-thrust belts is the result of the interplay of two major properties of the subduction system: (1) dynamics of plate interaction at the subduction zone, and (2) thermomechanical properties of the South American lithosphere.

The first factor is related to changes in convergence direction between the Nazca and South American plate, the respective velocities of each plate, and the age of the subducted slab (Jarrard, 1986; Sobolev and Babeyko, 2005; Oncken et al., 2006). In particular, the development of flat-slab segments is a key feature of the Andean subduction system, and has been proposed to be a first-order control on orogenesis (Ramos, 2010). The influence of the upper plate is related to preexisting weaknesses and to crustal structure. Inherited structures such as ancient faults and suture zones can be reactivated during orogenesis, affecting the dynamics and morphology of orogenic belts (Allmendinger et al., 1983; Kley et al., 1999; Ramos et al., 2002; Pearson et al., 2013). Thermal flux and variations in crustal composition and predeformation thickness control the rheological behavior of the upper plate, playing a determinant role in the configuration of the Andean orogen (Tassara et al., 2006). According to Jordan et al. (1983), attempts to determine the role of the plate interactions must first filter out the influence of upper plate inherited structures.

Therefore, establishing the importance of upper plate characteristics in the different Andean segments is an important aspect to understand subduction-related orogenesis. To address this issue, we constructed a cross section in the Malargüe fold-and-thrust belt at 35°S, in the transition between the Pampean flat-slab developed between 27° and 33°S (Ramos et al., 2002) and the segment of normal subduction developed to the south. The change in dip of the subducted Nazca plate has been assigned a major control in the structure of the Andes (Jordan et al., 1983; Ramos et al., 2002). Deformation of the foreland to a distance of 700 km from the trench and enhanced shortening in Andean thrust belts (>120 km) have been attributed to increased plate coupling and the development of brittle-ductile transitions in the foreland due to the migration of magmatism in the flat-slab

Geosphere; June 2014; v. 10; no. 3; p. 585–609; doi:10.1130/GES00939.1; 18 figures; 1 supplemental file.
Received 12 April 2013 ♦ Revision received 24 February 2014 ♦ Accepted 8 April 2014 ♦ Published online 25 April 2014

segment (Ramos et al., 2002). In contrast, the normal subduction segment shows a narrow orogen and a southward decrease in shortening (<60 km). However, a Miocene flat-subduction zone has been proposed to drive orogenic development in the currently normal subduction segment (Folguera et al., 2006).

In this framework, the aim of this contribution is twofold. First, we analyze the pre-Andean controls on the deformation in the transitional zone between the flat-slab and the normal subduction segments, evaluating structural models based on (1) tectonic inversion of preexisting faults and (2) newly formed Andean thrusts. With the results of this analysis, we address the second objective, which is to discuss the tectonic processes responsible for Andean orogenesis in this segment. The conclusions we present have implications for other studies of subduction-related orogenic processes and tectonic reactivation of inherited structures.

GEOLOGIC SETTING

The Malargüe fold-and-thrust belt was defined by Kozlowski et al. (1993) as a basement-involved belt composing the Andes of the southern half of the province of Mendoza (34°S–36°S), Argentina (Fig. 1). A major feature of the belt is a southward decrease in shortening (Kozlowski et al., 1993; Manceda and Figueroa, 1995; Ramos et al., 1996; Giambiagi et al., 2009a). Kozlowski et al. (1993) divided the belt longitudinally in three sectors: inner (western), middle, and outer (eastern) (Fig. 1B). In the inner sector, basement is involved in the deformation along its entire length, whereas the middle and outer sectors have a thin-skinned deformation, restricted to the Mesozoic–Cenozoic cover, in their northern parts.

The basement-involved character of the Malargüe fold-and-thrust belt was recognized since the work of Gerth (1931). However, different models have been proposed for the mechanism of basement deformation. Some have interpreted the deformation as the result of inversion of Mesozoic normal faults (Manceda and Figueroa, 1995; Uliana et al., 1995; Kley et al., 1999; Giambiagi et al., 2005, 2008), whereas others have proposed the development of new basement-involved Andean thrusts (Dimieri, 1997; Turienzo, 2010). A hybrid model including both kinds of structures has also been used (Giambiagi et al., 2009a).

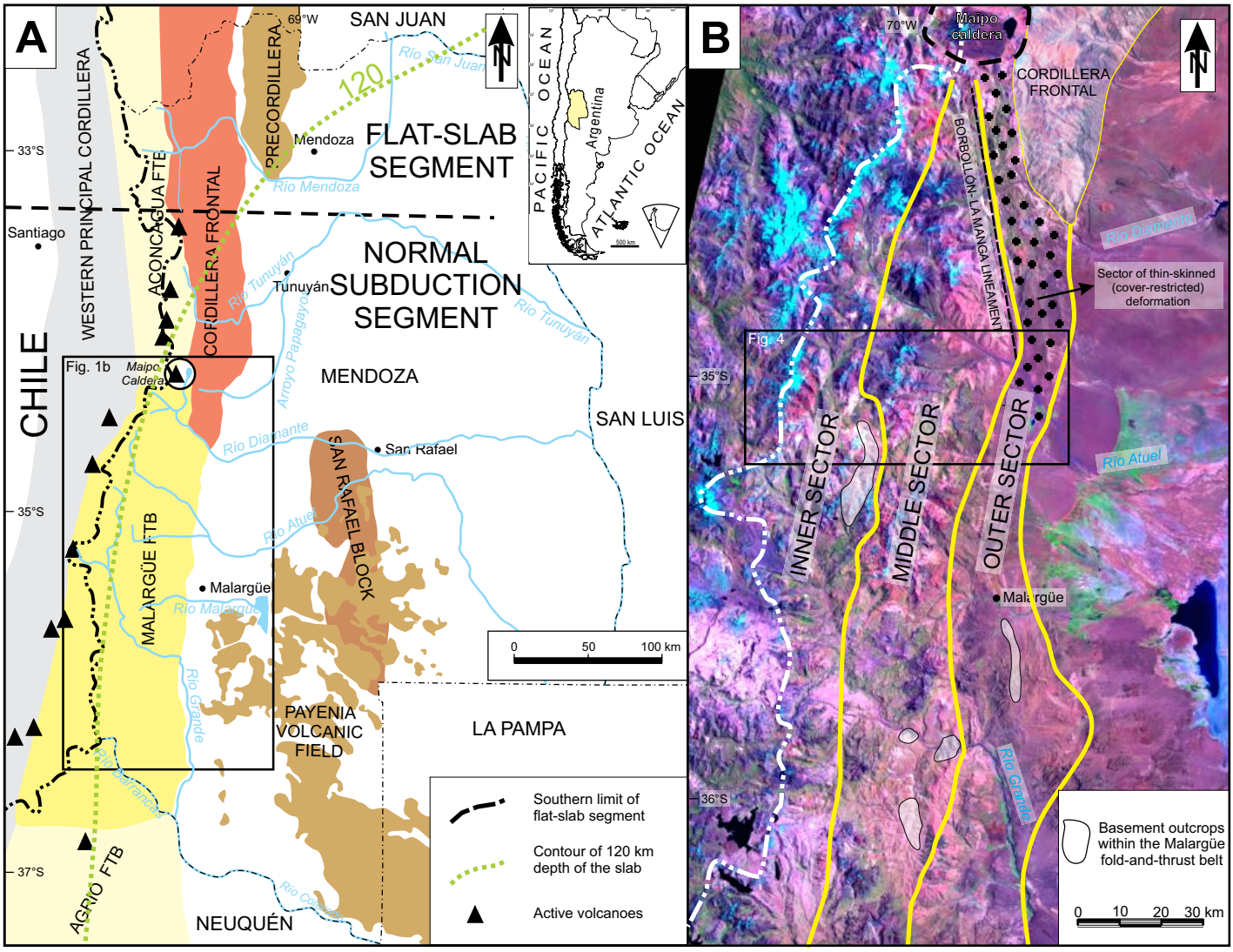

Figure 1. (A) Morphostructural units developed in the study area, province of Mendoza (modified from Kozlowski et al., 1993). (B) Structural sectors of the Malargüe fold-and-thrust belt over LANDSAT image (band combination RGB 742).

The model of tectonic inversion proposes reactivation of the Late Triassic to Early Jurassic normal faults that controlled the initial depocenters of the Neuquén Basin (Charrier, 1979; Gulisano, 1981; Uliana and Biddle, 1988; Manceda and Figueroa, 1995; Legarreta and Uliana, 1996, 1999; Lanés, 2005; Lanés et al., 2008; Giambiagi et al., 2009b; Bechis et al., 2010, and many others). Additional Late Jurassic extensional reactivation has also been proposed for some areas of the basin, including the study area (Mescua et al., 2008). Orientations of the normal faults vary throughout the Neuquén Basin (see Fig. 2A), but north of 36°S, master faults that bound depocenters strike between north-northwest and north-northeast (Giambiagi et al., 2009b). These orientations are suitable for inversion in the contractional Andean stress field with a regional maximum horizontal stress oriented east-west (Mescua and Giambiagi, 2012). Ramos et al. (1996) noted a link between the Mesozoic extensional depocenters and areas of basement-involved Andean deformation in the high Andes of the Mendoza and San Juan provinces of Argentina. In the northern part of the Malargüe fold-and-thrust belt, an inner sector of basement-involved deformation and an outer sector of cover deformation are separated by the Borbollón–La Manga lineament, which was interpreted (by Giambiagi et al., 2005, 2008) as the master fault of the Mesozoic Atuel depocenter of the Neuquén Basin (Fig. 2), based on the thickness and facies changes of the syn-extensional deposits.

In contrast, the model of exclusive Andean-age thrusts proposes that newly formed thrusts within the basement are responsible for deformation and uplift in the Malargüe fold-and-thrust belt (Dimieri, 1997; Turienzo, 2010). This model is based on sectors of the belt where basement structures transfer high amounts of shortening to the cover, a feature that cannot be explained through tectonic inversion that produces smaller amounts of horizontal shortening (Ramos et al., 1996; Dimieri et al., 1997). In other areas of the belt, such as near the locality of Bardas Blancas (35°51′S) no major extensional Mesozoic depocenters were developed, and consequently tectonic inversion is limited (Dimieri, 1997; Di Carlo and Cristallini, 2007).

METHODS

An extensive field survey of the Malargüe fold-and-thrust belt at 35°S was completed to characterize the main structures of the belt and stratigraphic variations. To characterize fault zones in the study area, units cropping out on the hanging walls and footwalls were mapped, attitudes of bedding planes were systematically measured, and, where possible, kinematic indicators, consisting of striae and slickenlines from slip planes, were measured. Kinematic data were analyzed using the FaultKinWin software (FaultKinWin version 1.2.2; see updated FaultKin 7 at http://www.geo.cornell.edu/geology/faculty/RWA/programs.html) to calculate P (pressure) and T (tension) axes and principal axes of mean incremental deformation using linked Bingham distribution statistics, in order to estimate the slip direction on the fault zone. Fold geometries were described with the aim of interpreting the processes responsible for their origin (i.e., buckling, fault-propagation folding, fault-bend folding, detachment folding). Timing relations of faults and folds were obtained based on crosscutting relationships with dated igneous rocks (Baldauf, 1997; Sruoga et al., 2008, 2009), and on relations with synorogenic deposits (Mescua et al., 2013).

Field work was complemented with analysis of gravimetric data available for the study area (see the Supplemental File[1]). In particular, we applied the Euler deconvolution technique to Bouguer anomaly values (Reid et al., 1990; Roy et al., 2000; Mushayandebvu et al., 2004) in order to interpret the subsurface continuation of lineaments observed in the surface. Euler's deconvolution is based on the application of Euler's homogeneity equation in a mobile window for a fixed width and parameter termed structural index. The structural index is associated with the geometry of the generating source, and is represented by a varying number from 0.5 to 2 (Roy et al., 2000). For this study, the best results were obtained with a structural index of 0.5 (Barbosa et al., 1999; Roy et al., 2000; Cooper, 2006). Window width was adapted to the structural dimensions of the target. In this study, we used a window width of 10 km over a 1 × 1 km grid, considering a 10% margin of error. For each position of the mobile window, a linear system of overestimated equations is used to obtain the position and depth of the sources. Linear features obtained by joining the solution points of the technique can be interpreted as deep geological structures.

Using the information obtained by these methods, we constructed a balanced cross section, which was forward-modeled using 2DMove software (Midland Valley Exploration Ltd.; http://www.mve.com/software/legacy_2dmove). The predeformation geometry, reconstructed from field data (see Structural Model and Balanced Cross Section discussion), was used to begin the modeling. We used the trishear algorithm implemented in 2DMove for deformation at fault tips (Erslev, 1991; Allmendinger, 1998). Trishear permits modeling a wide range of fold geometries by varying the trishear angle, the deformation field symmetry, and the fault propagation to slip (P/S) ratio. By varying this ratio, the trishear algorithm can generate detachment folds (P/S ~ 0), fault-propagation folds (low values of P/S) and fault-bend folds (P/S > 10), because these geometries can be viewed as points along a continuum of P/S values (Allmendinger et al., 2004). Backlimb deformation was accommodated using either fault-parallel flow or inclined shear with a shear angle between –20° and –30°, in order to model the observed geometry of the Mesozoic beds in each structure.

STRATIGRAPHY OF THE STUDY AREA

The stratigraphic record of the study area (Fig. 3) can be divided into (1) pre-Jurassic basement rocks, (2) Mesozoic sedimentary strata of the Neuquén Basin, (3) Cenozoic volcanic and plutonic rocks and volcaniclastic synorogenic deposits, and (4) Quaternary deposits, which will not be described in this contribution.

Pre-Jurassic Basement

One of the few outcrops of Paleozoic rocks in the Cordillera Principal of the province of Mendoza is found in the study area. Aparicio (1950) first described the quartzites, schists, and slates, which were later assigned to the Arroyo Mendino Formation (Nullo et al., 2005). A late Paleozoic age is assigned to this unit based on correlation with rocks of similar lithologies found in the Cordillera Frontal, north of the study area. The Arroyo Mendino Formation underlies and is intruded by the Permian to Early Triassic Choiyoi Group, a volcanic and plutonic unit of wide distribution in the Andes of Mendoza province (Llambías et al., 1993). In the study area, the Choiyoi Group comprises andesites, dacites, and rhyolites.

Mesozoic Sedimentary Succession of the Neuquén Basin

During the Mesozoic, the study area was part of the Neuquén Basin (Fig. 2), a retroarc extensional basin developed since the Late Triassic (Legarreta and Uliana, 1999). The infill of the basin consists of as much as 7 km of alternat-

[1]Supplemental File. The Supplemental File includes details about the gravity data used and its interpretation, the uncertainty in shortening values derived from the balanced cross-section, and an analysis of the effect of taking into account magmatic additions in crustal balancing. If you are viewing the PDF of this paper or reading it offline, please visit http://dx.doi.org/10.1130/GES00939.S1 or the full-text article on www.gsapubs.org to view the Supplemental File.

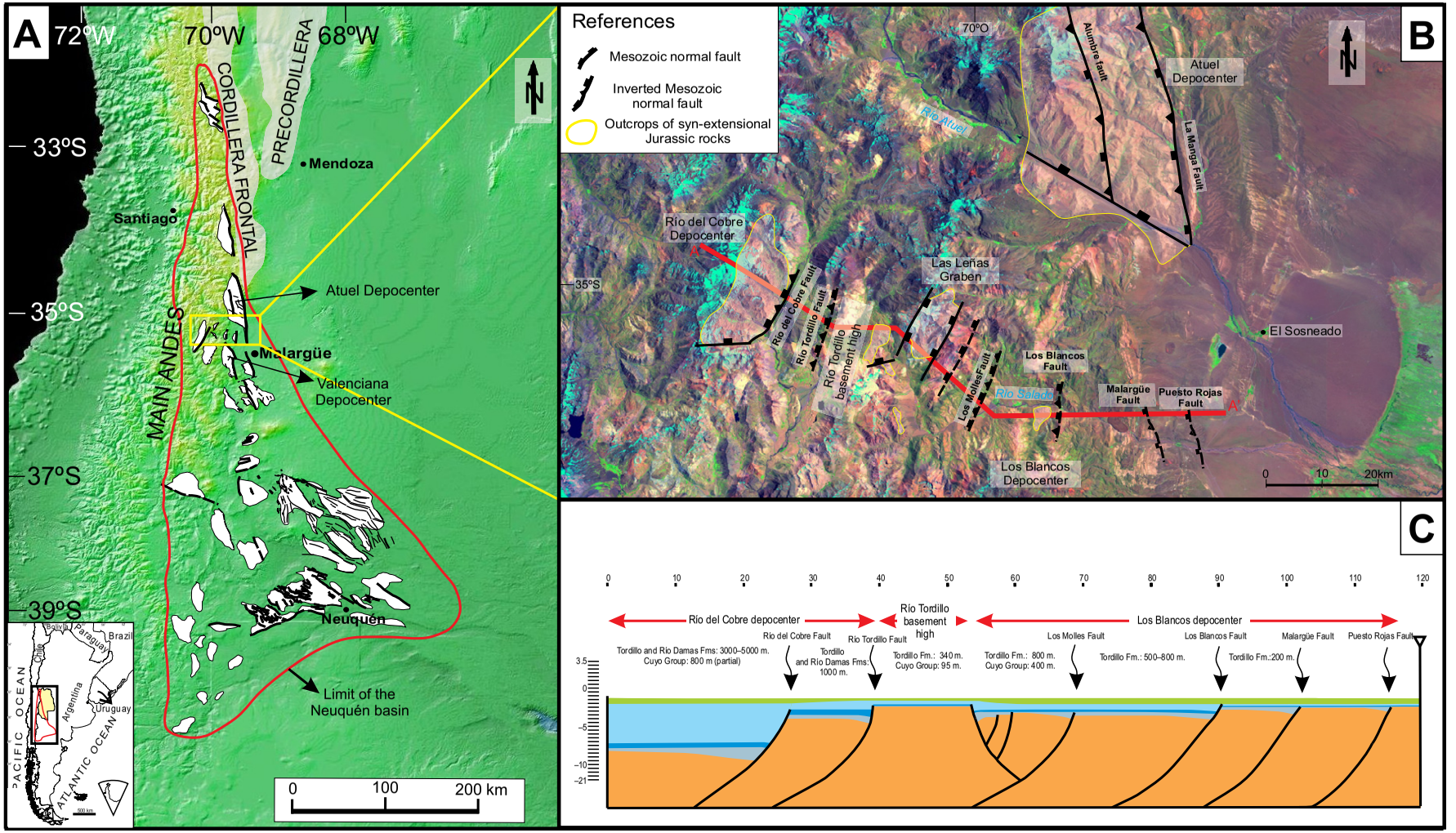

Figure 2. (A) Location of the Neuquén Basin (in red), and initial extensional depocenters (in white) over a topographic image. (B) Locations of normal faults and initial depocenters of the Neuquén Basin at 35°S. Present outcrops of the synextensional Early to Middle Jurassic units are shown. Red line A–A′ shows the trace of the cross section of Figure 3C. (C) Cross section shows the geometry of the Neuquén Basin at 35°S prior to Andean compressional deformation.

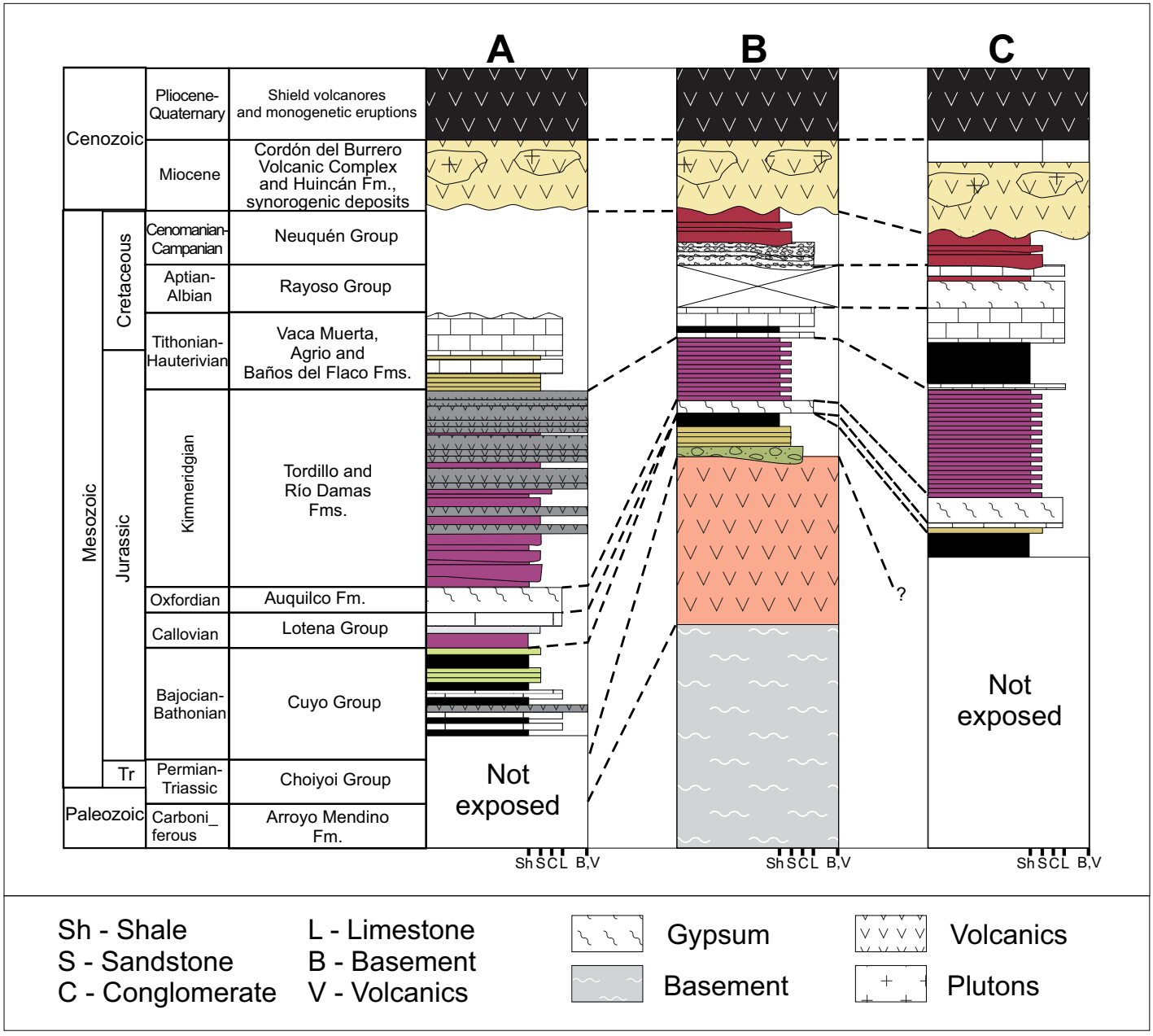

Figure 3. Simplified stratigraphy of the Andes at 35°S (not to scale). Column A corresponds to the western part of the study area (Río del Cobre depocenter), B corresponds to the central part (Las Leñas basement high), and C corresponds to the eastern part (Los Blancos depocenter). Colors correspond to rock colors in outcrop. Tr—Triassic.

ing marine and continental strata deposited in response to a combination of tectonic activity, eustasy, and volcanic activity in the arc, which also controlled the connection of the basin with the western paleo–Pacific Ocean (Legarreta and Uliana, 1996).

At 35°S, the basin comprises two depocenters (western Río del Cobre and eastern Los Blancos) separated by a basement high (Gerth, 1931; Davidson and Vicente, 1973; Legarreta and Uliana, 1999; see Fig. 2). This geometry developed during initial stages of the Neuquén Basin, when isolated, fault-controlled subbasins formed during an extensional period in Late Triassic–Early Jurassic time (Gulisano, 1981; Manceda and Figueroa, 1995). At this latitude the oldest rocks of the Neuquén Basin correspond to Early–Middle Jurassic marine rocks of the Cuyo Group, which contains both synextensional and postextensional deposits (Legarreta and Uliana, 1999). The Cuyo Group is conformably covered by Callovian to Oxfordian shallow-marine deposits (Lotena Group), which grade upward from red shales with minor sandstones to limestones (Davidson and Vicente, 1973). Later in the Oxfordian, a regional episode of desiccation across the basin is marked by gypsum of the Auquilco Formation, which has a maximum thickness of 400 m. The Kimmeridgian Tordillo and Río Damas Formations show a marked continentalization of the Neuquén Basin and were deposited in predominantly fluvial environments (Legarreta and Uliana, 1999) during a

period of active extension in the northern sector of the basin (Cegarra and Ramos, 1996; Pángaro et al., 1996; Giambiagi et al., 2003; Charrier et al., 2007; Mescua et al., 2008). The Vaca Muerta, Agrio, and Baños del Flaco Formations were deposited during Tithonian marine ingression (Legarreta and Uliana, 1999; Klohn, 1960). In the eastern part of the study area, these units are covered by evaporites and limestones of the Barremian to Aptian Rayoso Group (Nullo et al., 2005). A change from retroarc to foreland basin is recorded in the Late Cretaceous redbeds of the Neuquén Group, pointing out the first episode of Andean exhumation at the studied latitudes (Tunik et al., 2010; Mescua et al., 2013). The paleogeography of the rocks of the Neuquén Basin in the study area is discussed in further detail in the following.

Cenozoic Volcanic and Plutonic Rocks

The oldest Cenozoic volcanic rocks recognized in the study area are 18 Ma andesites of the Cordón del Burrero Volcanic Complex (Sruoga et al., 2008). Andesites, diorites, rhyolites, and basaltic dikes assigned to this volcanic complex show an intermediate geochemistry between arc and retroarc magmatism and have Ar/Ar total rock ages of 18–14 Ma (Sruoga et al., 2008). Volcanic and plutonic rocks that intrude or cover the Cordón del Burrero Volcanic Complex are assigned to the Huincán Formation. These rocks correspond to andesites, rhyolites, diorites, monzonites, and granites with a clear arc signature (Nullo et al., 2002) and have Ar/Ar hornblende ages from 12 to 6 Ma (Baldauf, 1997; Sruoga et al., 2009). Synorogenic volcaniclastic deposits coeval with the Huincán Formation volcanism, assigned to the Loma Fiera Formation (Baldauf, 1997; Combina and Nullo, 2000), are preserved in the cores of synclines in the eastern part of the study area. Pliocene to Holocene volcanic rocks are found in the study area, as large eruptive centers and small monogenetic cones (Fig. 4; Sruoga et al., 2005).

MAIN STRUCTURES OF THE MALARGÜE FOLD-AND-THRUST BELT AT 35°S

The westernmost part of the study area is characterized by outcrops of Mesozoic strata of the Neuquén Basin (Fig. 4). In the northwest of the study area, a large north-plunging anticlinorium is developed, in which Kimmeridgian and younger units form a large anticline of 10 km wavelength, cut along its eastern flank by the Río del Cobre fault zone (Fig. 4). In the core of this anticline, underlying Jurassic units are complexly deformed by thrusts and folds of smaller wavelengths. To the south, the anticlinorium and fault zone abut the Santa Elena lineament (Fig. 4).

The Río del Cobre fault zone, one of the major structures within the cross section (Figs. 4 and 5), is a north-northeast–striking, high-angle (~60°W) reverse fault zone that is as much as 600 m wide. Fault rocks are intensely deformed red shales of the Lotena Group, gypsum of the Auquilco Formation, and sandstone blocks of the Cuyo Group (Fig. 5A). The fault places the Middle Jurassic Cuyo Group over Oxfordian to Kimmeridgian rocks, with an estimated reverse displacement between 3000 and 5000 m that decreases toward the north. A kinematic study of minor slip structures in the fault zone indicates reverse dip displacement of the fault and little or no strike-slip component (Fig. 5B).

Deformation of the Cuyo and Lotena Groups west of the Río del Cobre fault zone presents two contrasting styles. In the northernmost part of the anticlinorium, the Middle Jurassic units are folded in a series of regular open anticlines and synclines with wavelengths of ~3 km (Fig. 6). In the southern part of the anticlinorium, beds of the Cuyo Group are deformed by imbricate thrust faults and associated folds (Fig. 7). Two main thrusts are observed. The western thrust shows a series of ramps and flats, including local juxtaposition of a hanging-wall ramp on a basal flat, suggesting out-of-sequence thrusting.

Farther south, beds of the Cuyo Group and the Río del Cobre fault zone abut a marked east-west Santa Elena lineament, which extends for 20 km in the western part of the study area (Fig. 4). In order to examine if the Santa Elena lineament corresponds to a subsurface structure, Bouguer gravity data were analyzed using the Euler deconvolution technique (Reid et al., 1990; Roy et al., 2000; Mushayandebvu et al., 2004). Solutions of Euler deconvolution that reflect the subsurface continuation of the Santa Elena lineament shown in Figure 4A correspond to a >15-km-deep lineament that marks an important upper crustal structure, which bounds two blocks with contrasting densities. The subsurface boundary is located 7 km north of the surface expression of the lineament, indicating that the boundary dips 65° to the north.

In the southwestern part of the study area, the outcrop level is higher than in the northwest, even though the altitude is lower. The Lotena Group and Auquilco Formation are intensely deformed into a series of tight anticlines and synclines with wavelengths of ~1 km (Fig. 8A). Folds in this sector trend north to north-northeast and are slightly sinuous. Along strike, folds widen and narrow, and are locally overturned as a result of the flow of the ductile units within fold cores. Box fold geometries are widespread (Fig. 8B). In one of the pioneering studies of this part of the Andes, Burckhardt (1900) had already recognized the structural complexity of this sector, and described a fold with the shape of an inverted bottle in the Laguna de las Cargas (Fig. 8). These observations indicate detachment folding facilitated by ductile behavior of lower Lotena Group red shales, which flowed into anticline cores and out of synclines.

Toward the east, between the Cobre and Tordillo Rivers, deformation of the Jurassic and Cretaceous units is characterized by folding (Fig. 4). The main structure is a north-northeast–trending syncline (Mescua et al., 2010) that undulates and intersects with north-northwest–trending folds, giving rise to a type 2 interference pattern (Ramsay, 1967).

The Las Leñas basement block was exhumed in the central sector of the study area (Fig. 4). Overlying Jurassic and Cretaceous units are only slightly deformed (Fig. 9), in contrast with the rest of the study area. Basement was uplifted along the north-striking, west-dipping Las Leñas thrust and cores a large anticline with eastern vergence (Fig. 10). A 65°–45° dipping frontal limb contrasts with a 15°–20° dipping backlimb in the Cuyo Group cover. The basement acted as a rigid block, with folding developed in the front (east) of the thrust. To the north and south of the study area, the fault slip decreases and the basement block plunges in both directions.

Where the Las Leñas fault reached the Mesozoic sedimentary succession, displacement transferred to the cover folds using weak units as detachment levels. Fold trends vary from north-northeast in the north to north-south in the south (Figs. 4 and 11). In the north, the detachment level is located in shale and limestone beds of the Cuyo Group, whereas in the south, the detachment level is in gypsum of the Auquilco Formation.

The eastern sector of the study area displays multiple north-trending folds in Mesozoic sedimentary cover, locally cut by faults (Fig. 4). The Los Morros fault (Kozlowski et al., 1984) placed the Vaca Muerta Formation over the Neuquén Group, but is mostly covered by Quaternary deposits. The main structure in this eastern sector corresponds to the 4-km-wavelength Los Blancos anticline, which is cored by the Cuyo Group (Fig. 4). A syncline developed to the east preserves Neuquén Group and Cenozoic synorogenic deposits (Fig. 4). East of these folds, a sector of smaller scale structures is found, characterized by thrusts and tight folds with 0.5–1 km of wavelengths, detached in gypsum of the Auquilco Formation and black shales of the Vaca Muerta Formation (Giampaoli et al., 2002).

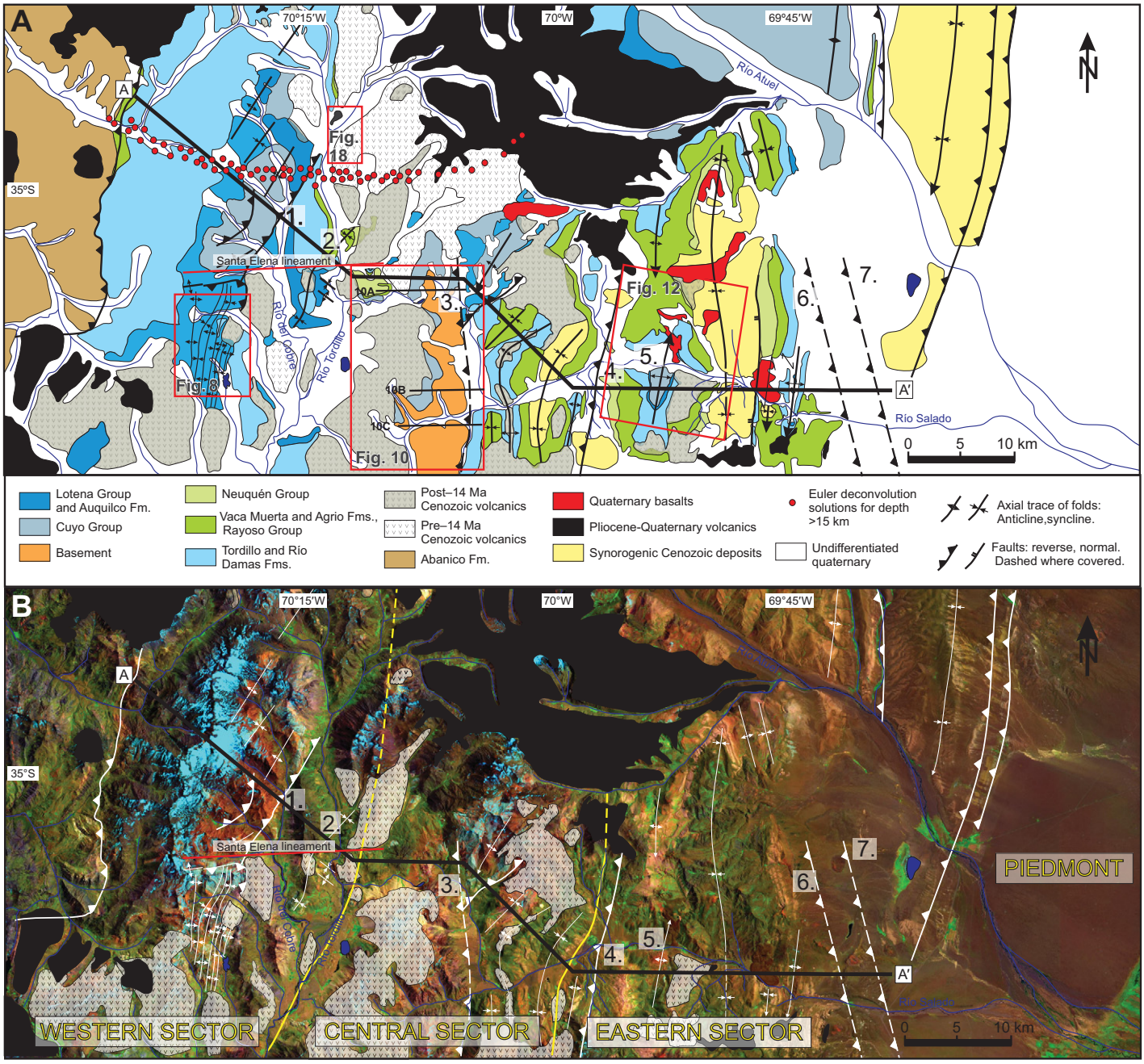

Figure 4. (A) Simplified geologic map of the Malargüe fold-and-thrust belt at 35°S. Location is in Figure 1. Red boxes indicate the locations of Figures 8, 10, 12, and 18. (B) Division in sectors of Kozlowski et al. (1993), over LANDSAT satellite image (band combination—RGB 742). The line A–A′ shows the trace of the balanced cross section (see Fig. 14). Numbers indicate some of the main structures: (1) Río del Cobre fault, (2) Río Tordillo syncline, (3) Las Leñas fault, (4) Los Molles fault, (5) Los Blancos anticline, (6) Malargüe fault, and (7) Puesto Rojas fault.

The frontal structures of the fold-and-thrust belt at these latitudes, the Malargüe and Puesto Rojas faults, have been documented in seismic lines and boreholes (Kozlowski et al., 1993; Giampaoli et al., 2002; Rojas and Radic, 2002). The faults offset basement and continue upward into anticlines in the Mesozoic sedimentary cover.

STRUCTURAL MODEL AND BALANCED CROSS SECTION

Based on the structural model presented in the following, and ages of progressive deformation described herein, we constructed a balanced cross section using 2DMove (see the Methods discussion). The construction of balanced cross sections in areas of tectonic inversion poses some difficulties, mainly due to the geometry of the extensional basin, which results in a complex stratigraphy of the infill. Depending on the level and quality of exposure, recognizing inverted faults may be straightforward or a very difficult task. In our case study, geometrical criteria used to recognize inversion, such as foot-

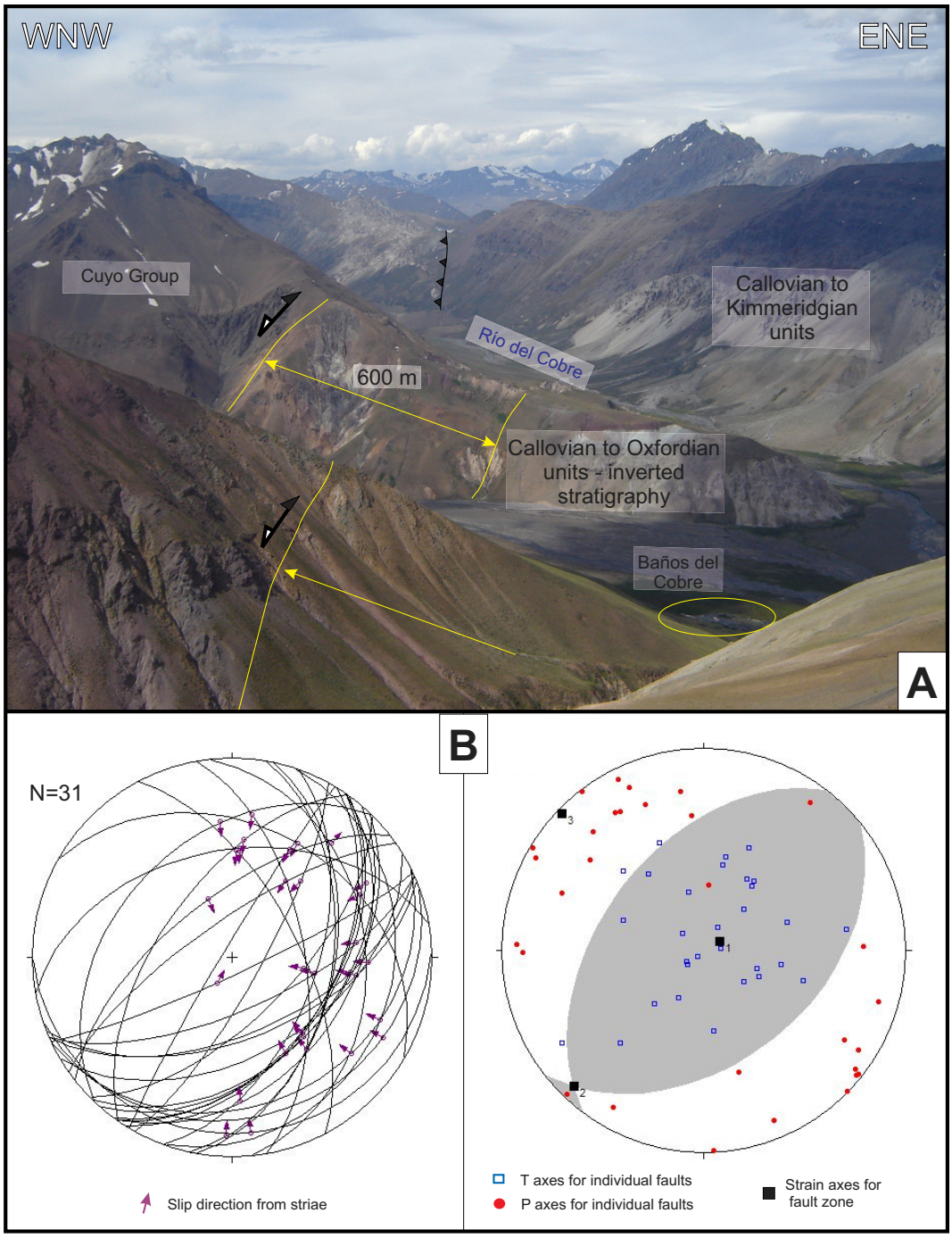

Figure 5. (A) The Río del Cobre fault zone. View is to the north-northeast. Note the thermal spring of Baños del Cobre and the block with inverted stratigraphy in front of the fault. (B) Kinematic analysis of the Río del Cobre fault zone, based on the measurement of striae on slip planes within the fault zone. On the left, fault planes with arrows showing striae and slip sense. On the right, calculated P (pressure) and T (tension) axes for individual faults and strain axes obtained using Linked Bingham statistics (1, 2, 3). The displacement obtained for the fault zone is represented as a focal mechanism, showing pure dip reverse displacement. Calculations and diagrams made with FaultKinWin (FaultKinWin version 1.2.2; see updated FaultKin 7 at http://www.geo.cornell.edu/geology/faculty/RWA/programs.html).

wall shortcuts (Hayward and Graham, 1989) and null points (Williams et al., 1989), could not be observed. Out-of-sequence deformation related to buttressing, as observed in the Río del Cobre depocenter (Figs. 6 and 7), was suggested as an indication of inversion by Hayward and Graham (1989). For other structures, we had to rely on variations in thickness and facies of Mesozoic synextensional strata to interpret inverted faults. In some cases, thickness variations are dramatic: for the Río del Cobre fault, the Tordillo and Río Damas Formations increase in thickness more than 2000 m (Fig. 2). In other cases, such as the Los Blancos fault, the increase is 300–500 m; this can be explained with a thrust, as proposed by Kozlowski et al. (1993). The argument for inversion of this structure is presented in the Discussion section. In settings like this, where inversion is likely but cannot be directly observed, a good approach is to assess the potential for reactivation of the preexisting structures using the Coulomb-Navier fracture and slip criteria, given their orientation and physical properties (Sibson, 1985). We have shown that in our case study, a small decrease in the coefficient of friction with respect to that of intact rock or a small increase in fluid pressure are sufficient to produce reverse reactivation of the normal faults of the Neuquén Basin (Mescua and Giambiagi, 2012).

Section-line changes strike locally from east-southeast to east-west to match interpreted transport directions of structures (Fig. 4). This implies

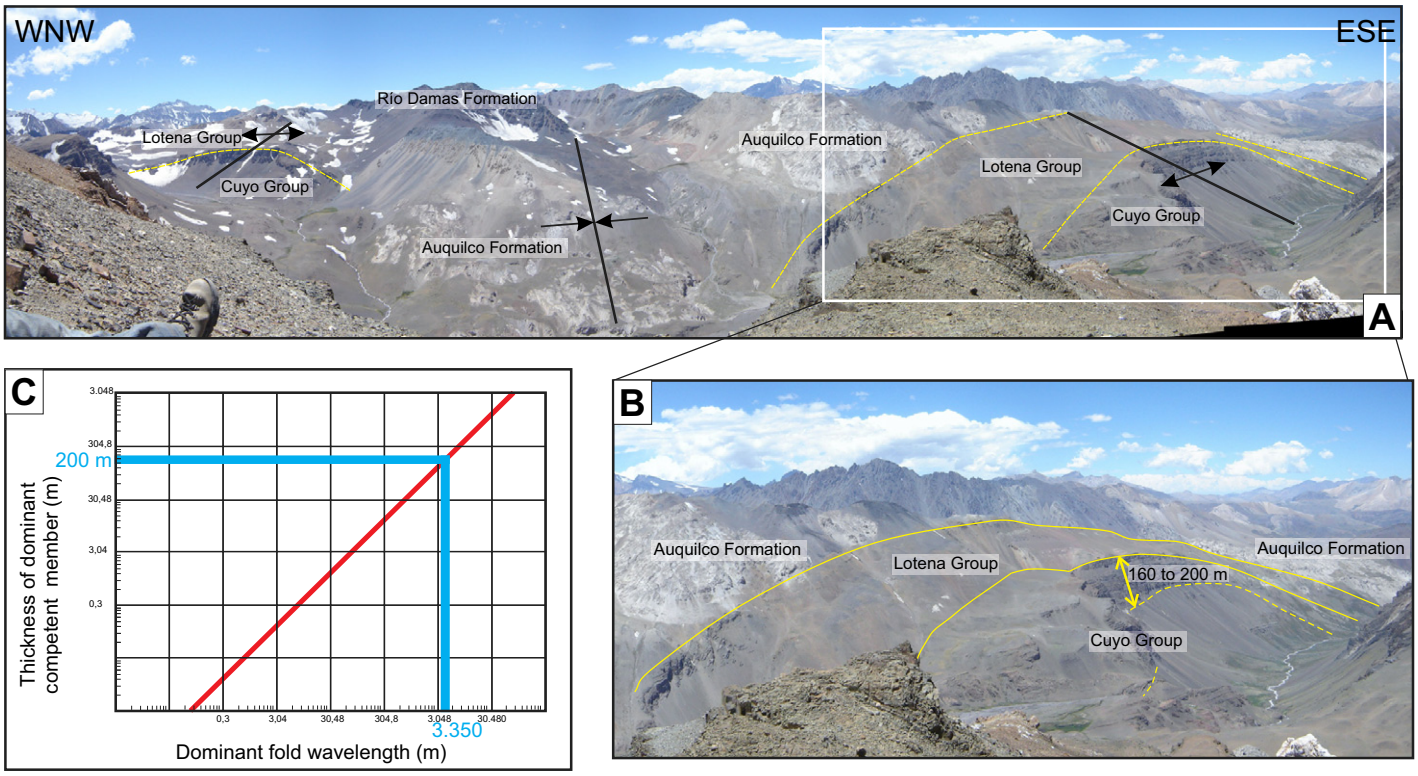

Figure 6. (A) Folds developed in the Mesozoic units of the Neuquén Basin in the northern sector of the Río del Cobre anticlinorium. Note the regular geometry and wavelength of the folds. Apparent convergence of axial traces is due to perspective. (B) Close-up of the eastern anticline with competent section outlined. (C) Relationship between thickness of competent unit and fold wavelength for multilayer buckling (from Currie et al., 1962). Data of Río del Cobre folds in light blue.

the assumption of pure dip-slip movement of the faults. If a strike-slip component was present in any of the structures, material motion out of the plane of the section would result in an increased uncertainty in estimated shortening. However, no significant strike-slip movements have been detected in the study area. Kinematic data for the north-northeast–striking Río del Cobre fault indicate dip-slip displacement (Fig. 5). The structures with the same strike east of the Las Leñas basement block, that we interpret as resulting from control by existing structures, continue southward into north-south structures without evidence for strike-slip deformation.

The western limit of the cross section is given by the contact between Mesozoic and Cenozoic along the El Fierro thrust (Charrier et al., 1996, 2002; Godoy et al., 1999). The El Fierro fault was active ca. 20 Ma during the inversion of the Eocene–Oligocene Abanico Basin west of the study area (Charrier et al., 1996, 2002), and may also have been active during out-of-sequence deformation between 9 and 3.5 Ma (Godoy et al., 1999). The eastern limit is the orogenic front.

The depth to detachment in the eastern part of the study area was taken as 10 km, similar to values from previous structural studies in the region (Giambiagi et al., 2008, 2009a) and geophysical modeling (Farías et al., 2010). A dip of ~2°W leads to a depth to detachment between 11 and 12 km at the western end of the cross section.

Geometry of the Half-Grabens of the Neuquén Basin

The Malargüe fold-and-thrust belt at 35°S presents a pattern in which structural style is related to the geometry of depocenters of the Neuquén Basin. Sedimentary strata of the Neuquén Basin are widely exposed in the western and eastern parts of the study area where Mesozoic depocenters were developed, whereas basement crops out in the central part of the study area that was a basement high during the Mesozoic. Taking this into account, we first reconstructed the geometry of the Neuquén Basin depocenters prior to initiation of Andean contractional deformation. Thickness variations of Mesozoic sedimentary deposits were characterized along the section line shown in Figure 4. An initial restoration of the main structures was carried out to construct the pre-Andean geometry of the basin (Fig. 2C), which was later adjusted during cross-section modeling. The basin included the western Río del Cobre depocenter (Fig. 2) composed of two half-grabens, the western of which has the thickest infill. The central part corresponded to the Las Leñas basement high, over which condensed sections of the Mesozoic units were deposited (Legarreta and Kozlowski, 1984). The eastern depocenter, called here Los Blancos depocenter (Fig. 2), was previously included within the Atuel-Valenciana depocenter by Manceda and Figueroa (1995). We differentiate this sector from the major Atuel and Valenciana depocenters developed to the north and south, respectively, because the sector at 35°S has a different geometry. It is composed of a series of minor half-grabens (Fig. 2C), whereas the Atuel and Valenciana present larger half-grabens (Giambiagi et al., 2009b). The Los Blancos anticline is interpreted to have formed at the northern termination of the Valenciana depocenter; however, minor half-grabens and grabens with relatively thin successions of synrift strata developed to the east and west of this structure (e.g., Las Leñas graben, Fig. 2) indicate a transitional sector with respect to the two main depocenters.

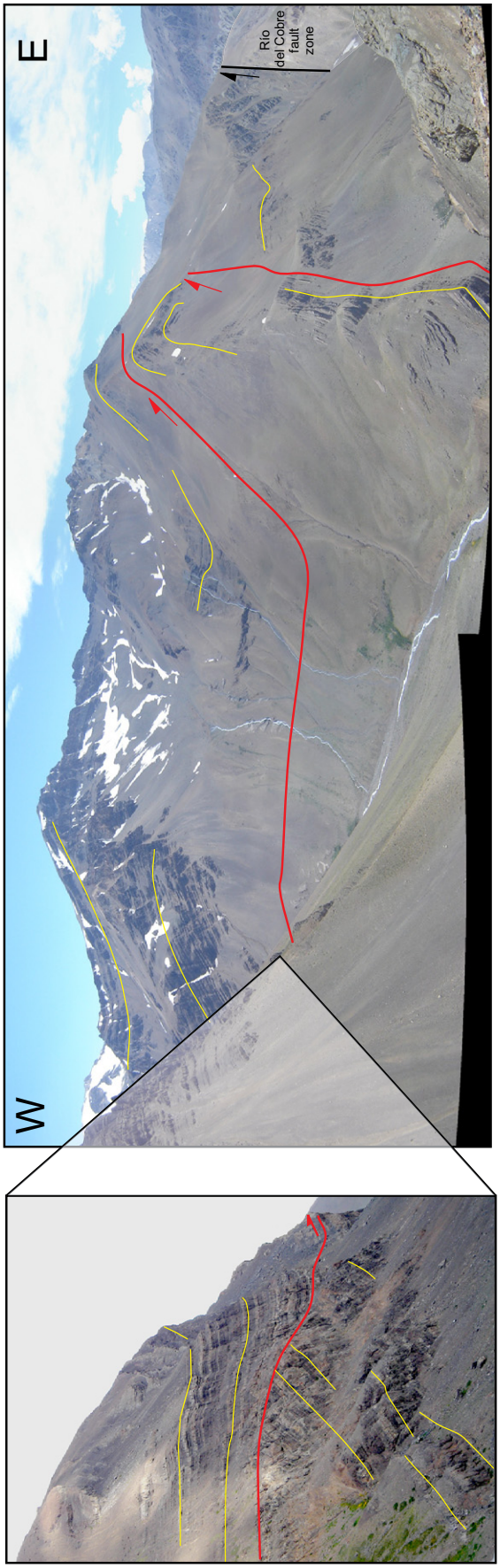

Figure 7. Thrusts developed in the Cuyo Group succession in the southern part of the Río del Cobre anticlinorium. Yellow lines trace beds, thrusts are in red. Close-up photograph on the left shows the out-of-sequence relationship along the western imbricate fault.

A significant point in the reconstruction is the location of the extensional faults of half-grabens and grabens. Changes in thickness and facies of the Jurassic rocks across faults may correlate with the inversion of Mesozoic structures during the Cenozoic deformation (Mescua and Giambiagi, 2012). The coincidence of large-wavelength folds (5–10 km) and thick successions of Early to Middle Jurassic rocks is interpreted to reflect inversion of half-graben bounding structures. Alternatively, these folds may reflect the locations and orientations of newly formed thrusts near preexisting normal faults (Nieuwland et al., 2000; Yagupsky et al., 2008).

Age of Deformation

Initial compressional deformation in the study area took place in the western part of the inner sector of the belt during the Late Cretaceous (Mescua et al., 2013) and is recognized at the regional scale (Tunik et al., 2010). In this sector, clast composition of the Late Cretaceous synorogenic conglomerates indicates exhumation and erosion of the Late Jurassic and Early Cretaceous strata, interpreted as an evidence for early uplift along the Río del Cobre fault (Mescua et al., 2013). After this deformation, an extensional episode restricted to the Chilean side of the Andes led to the development of the Abanico Basin during the Eocene and Oligocene (Charrier et al., 1996, 2002).

The main deformation in the Malargüe fold-and-thrust belt took place in the Miocene (Fig. 12), starting ca. 20 Ma in the Chilean Andes west of the study area, with the inversion of the Abanico Basin (Charrier et al., 1996, 2002). Within the study area, the inner sector of the belt was deformed between 20 and 16 Ma, as evidenced by syntectonic folded andesites of the Cordón del Burrero Volcanic Complex with Ar/Ar total rock ages of 17.9 ± 0.4 Ma and 17.2 ± 0.2 Ma, and undeformed rocks of the same unit with ages of 16.3 ± 0.1 Ma and 16.1 ± 0.2 Ma (Sruoga et al., 2008). The deformation advanced to the east, as shown by syntectonic dikes of 13.57 ± 0.12 and 13.43 ± 0.09 Ma intruded in the Los Blancos anticline, and the post-tectonic emplacement of the Los Morros intrusion in the core of an anticline at 12.4 ± 0.7 Ma (Ar/Ar hornblende ages of Baldauf, 1997). Synorogenic deposits of the Loma Fiera Formation that are preserved in synclines in the easternmost part of the belt were dated by Baldauf (1997) as younger than 10 Ma. Deformation in the Malargüe anticline, at the front of the Malargüe fold-and-thrust belt, started after 7 Ma and continued until 1 Ma (Silvestro et al., 2005). The Las Leñas fault presents out-of-sequence deformation that could not be dated (see following).

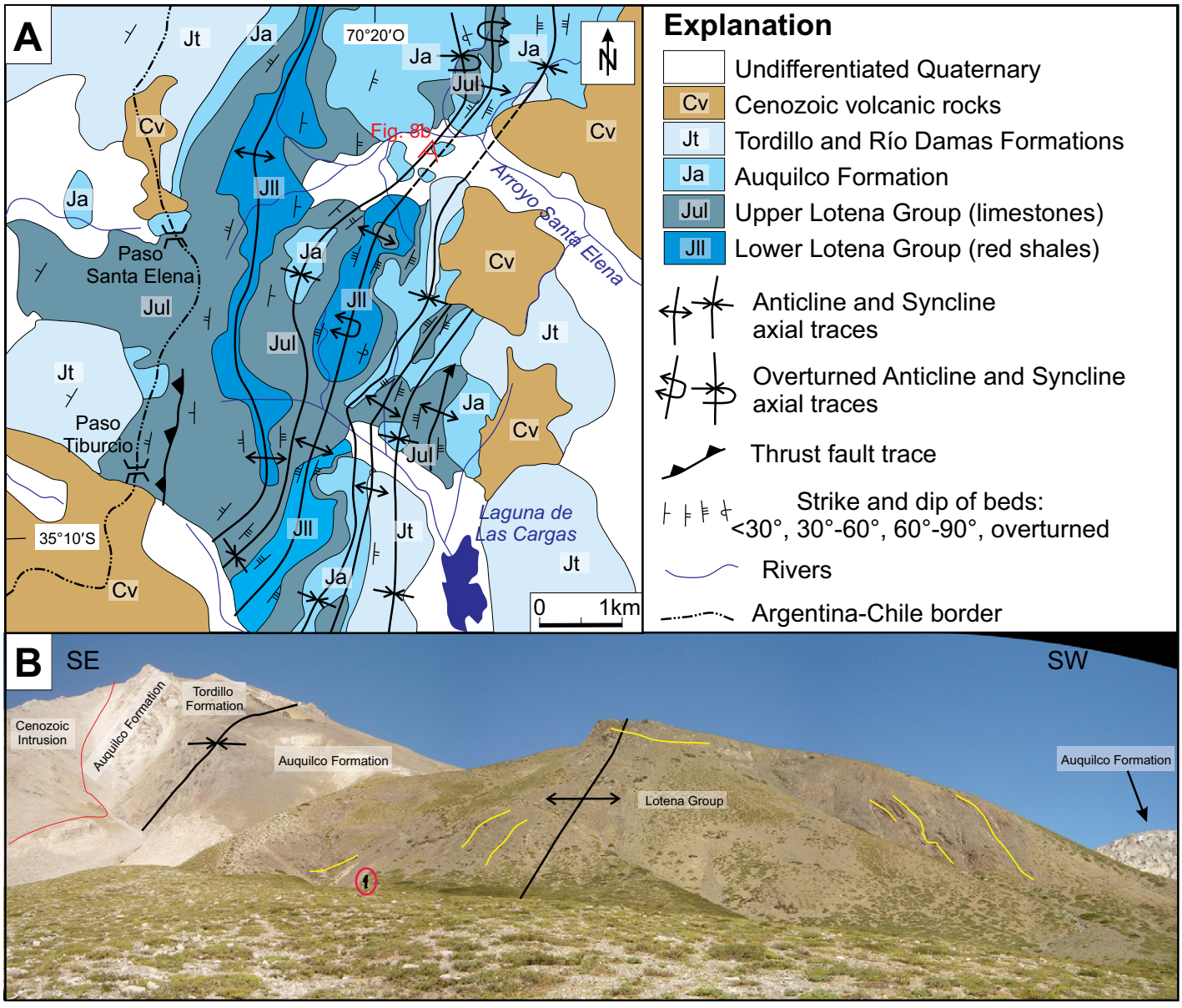

Figure 8. (A) Geologic map of the southwestern part of the study area. Note tightening and widening of the folds along strike, and changing geometry of folds from upright to inclined to overturned, features indicative of detachment folding. See Figure 4 for location. (B) An example of a detachment fold with box-fold geometry, location in A. Person for scale in the red circle.

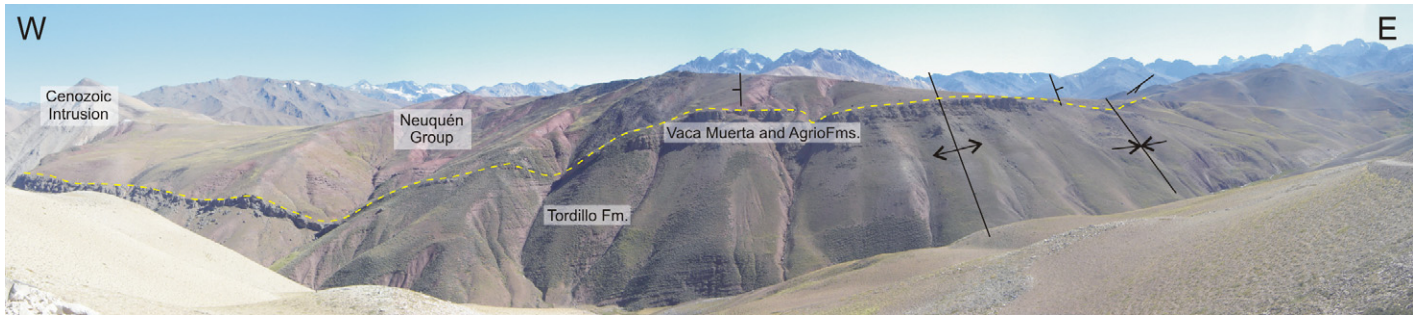

Figure 9. Mesozoic beds on top of the Las Leñas basement block display only limited, open folding, which contrasts with the structural style of the same beds in the rest of the study area.

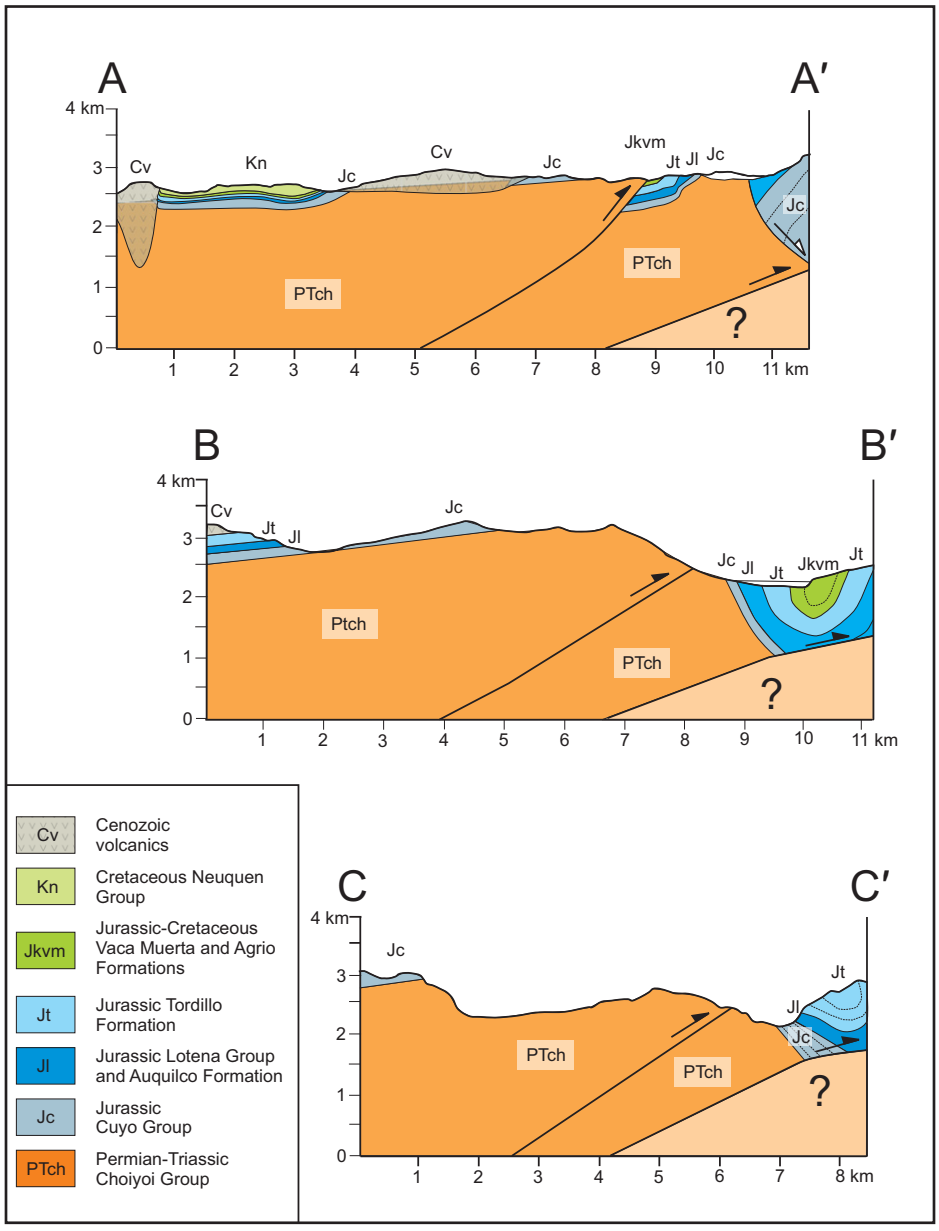

Figure 10. Schematic cross sections across the Las Leñas basement block (see Fig. 4 for location). The reverse faults are interpreted to join at depth. The eastern thrust transfers its displacement to the cover through a décollement level located within the Cuyo Group in section A–A′ and in the gypsum of the Auquilco Formation in sections B–B′ and C–C′. The western out-of-sequence thrust activated after the eastern one. Note that displacement on the western thrust decreases to the north, leading to lower altitude and exhumation in the A–A′ cross section.

Structural Model for Andean Deformation and Balanced Cross Section

The evolution of the deformation in the Malargüe fold-and-thrust belt modeled in 2DMove is shown in nine steps in Figure 13. Some structures with more limited shortening along the cross section likely correspond to inverted Mesozoic normal faults, such as the Río del Cobre fault (Mescua and Giambiagi, 2012). The high angle of this structure is a typical feature of normal faults (Fig. 5). In addition, an 800-m-thick succession of deep-marine facies of the Cuyo Group, representing the transition from synrift to postrift stages, is west of the fault. Even though this unit does not crop out immediately to the east of the fault, further east over the Las Leñas basement high, only 95 m of shallow-marine deposits are found (Fig. 13A). Extensional control on deposition of this unit has been widely documented in other localities (Manceda and Figueroa, 1995; Lanés, 2005; Giambiagi et al., 2008, 2009b; Bechis et al., 2010). The thickness of the Late Jurassic Tordillo Formation increases from 1000 m in the footwall of the Río del Cobre fault to between 3000 and 5000 m in the hanging wall, recording an extensional control that has also been documented at the regional scale (Fig. 13A). These observations suggest that the Río del Cobre fault was a normal fault during the Middle and Late Jurassic, and was reactivated as a reverse fault during Andean deformation. Furthermore, this can explain the north-northeast trend of the fault, oblique with respect to the Andean stress field, which varied between azimuths 76° and 83° (Somoza, 1998; Somoza and Ghidella, 2005).

According to this interpretation, internal deformation of the Cuyo and Lotena Groups, concentrated near the Río del Cobre fault zone, results from buttressing of the beds against the footwall basement. Different styles of deformation observed in these beds appear to be controlled by variations in the lithological characteristics of the Cuyo Group. In the northern part, shales are dominant, except for a 150–200 m section of sandstones that controlled buckling with fold wavelength correlated to thickness of the competent section (Currie et al., 1962; Fig. 6C). In contrast, in the southern part, the succession is dominated by sandstones, and deformation is mostly by thrusting (Fig. 7). The internal deformation of the Middle Jurassic rocks by buttressing against the basement step of the Río del Cobre fault is not represented in the cross section. We modeled the inversion of the Río del Cobre fault as a simple harpoon anticline (Yamada and McClay, 2004), following the geometry of the overlying Late Jurassic rocks.

The Santa Elena lineament (Fig. 4) was the southern termination of this depocenter, corresponding to either a normal fault or a transfer zone. To the south of the Santa Elena lineament, outcrops of Cuyo Group rocks are limited, and the deformation style in the Lotena Group rocks is markedly different from that developed in the north. The contrast in rock density at depth across the Santa Elena lineament recorded by gravity data is interpreted as a contact between different kinds of basement rocks. We interpret this density contrast as the existence of a normal fault that put Paleozoic rocks against the Choiyoi Group. The observed lineament and gravity contrast disappear to the east, where the Las Leñas basement high is located.

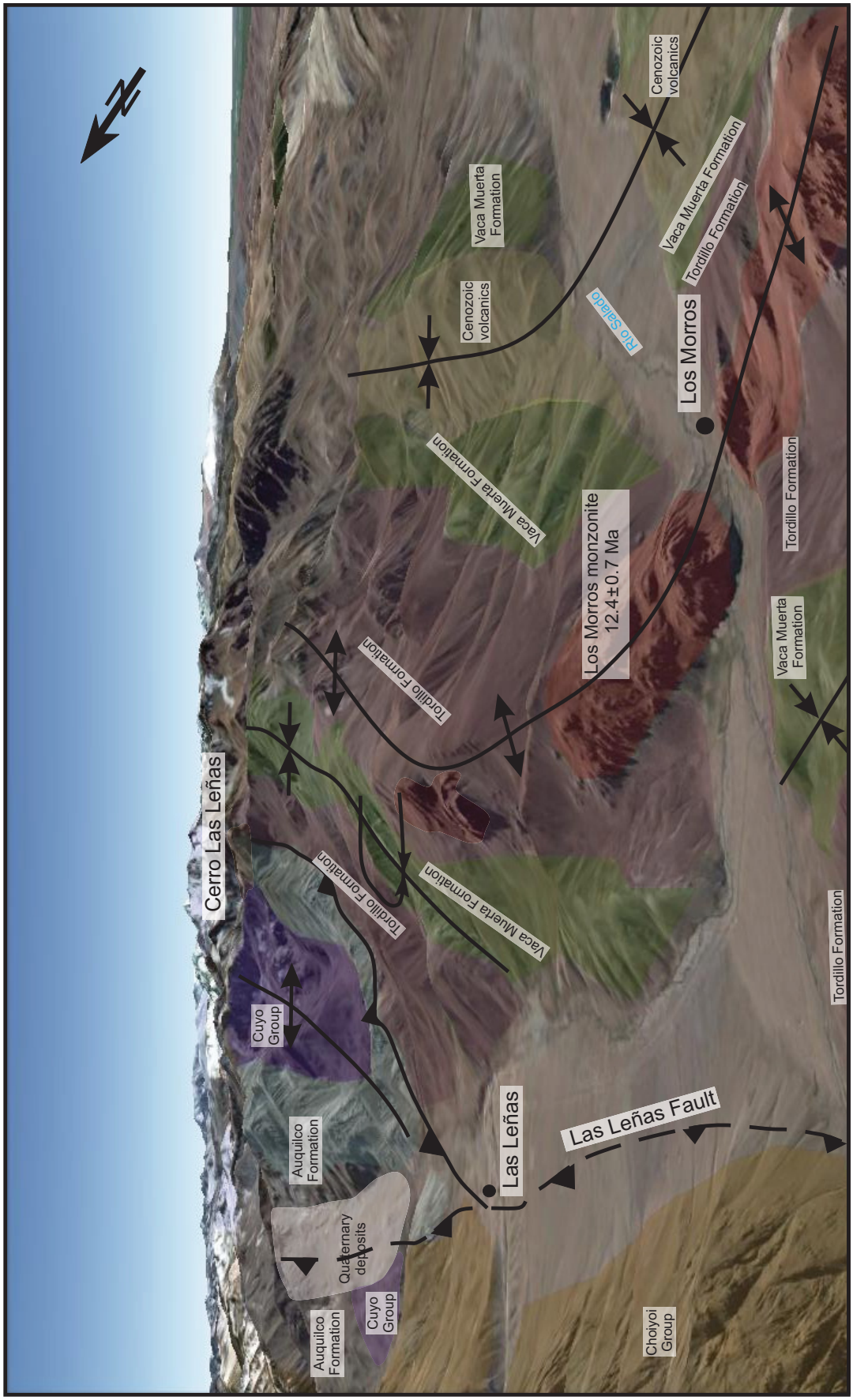

Figure 11. View to the north-northeast showing the frontal part of the Las Leñas basement block and the folds with control of the Mesozoic Las Leñas graben. Note the change in orientation of the eastern folds coincident with the presence of a 400-m-thick succession of Early to Middle Jurassic rocks. Geologic map over image from Google Earth.

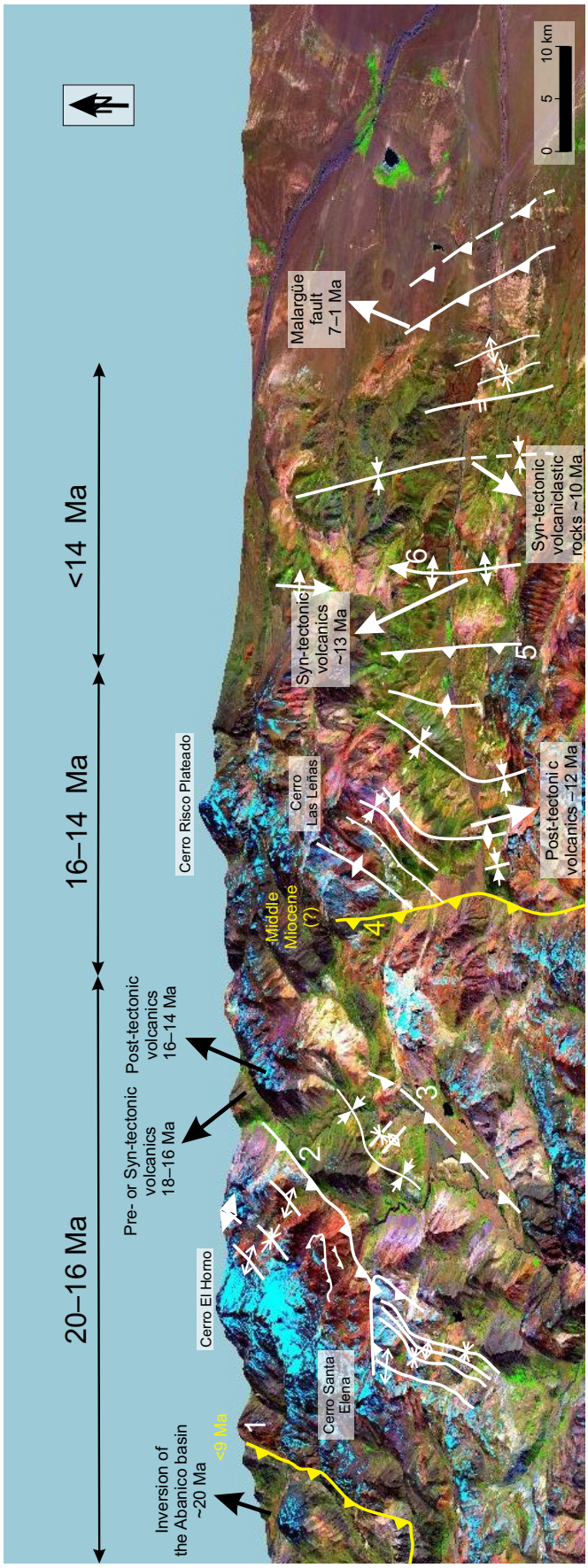

Figure 12. Timing of deformation across the Malargüe fold-and-thrust belt at 35°S. Structures in yellow indicate out-of-sequence deformation. See Figure 4 for location. Ages are from Charrier et al. (1996, 2002), Baldauf (1997), Silvestro et al. (2005), and Sruoga et al. (2008). Numbers indicate some of the main structures: 1—El Fierro fault, 2—Río del Cobre fault, 3—Río Tordillo fault, 4—Las Leñas fault, 5—Los Molles fault, and 6—Los Blancos anticline.

We propose a limited inversion of an inferred Mesozoic normal fault, the Río Tordillo fault, that is covered by Quaternary deposits and located east of the Río del Cobre fault (Figs. 13A, 13B). Across this structure, the Tordillo Formation thickness changes from 1000 m to 340 m. The Río Tordillo fault could also be an Andean thrust with a ramp location controlled by a preexisting normal fault. However, given that north-northeast–trending Mesozoic normal faults have a high potential for inversion in the Andean stress field (Mescua and Giambiagi, 2012), we favor the first interpretation.

We propose that the older normal faults of the Río del Cobre depocenter (Fig. 2) were inverted during Andean deformation in a way similar to that found by Marques and Nogueira (2008) in analog models, in which normal faults closer to the piston that generates the compression are more strongly inverted. In our case study, the western fault was also more important during extension, with higher displacement and a thicker sedimentary succession deposited in the western half-graben, which probably favored its inversion.

The Las Leñas Mesozoic basement high acted as a rigid basement block, with only limited deformation of the cover. Folding in the front of an east-verging, north-striking reverse fault is the most important deformation associated with this uplift (Fig. 13C). Following Kozlowski et al. (1993), we interpret the Las Leñas anticline as a fault-bend fold, generated when an Andean basement thrust transferred its displacement to the cover using flat detachment levels (Fig. 10). Kozlowski et al. (1993) noted the out-of-sequence transport of the anticline; a thrust cuts its eastern flank, affecting the cover folds south of the study area (Figs. 10 and 13D). The deformation of the cover took place with the generation of thrusts and folds (Fig. 11). These structures show changes in orientations and detachment levels from north to south. In the north, north-northeast–trending folds have a detachment in the Cuyo Group, whereas to the south, north-trending folds are detached in the Auquilco Formation. These are interpreted to result from interaction of the Las Leñas thrust with preexisting structures inherited from Mesozoic extension. The presence of a small depocenter with 400 m of the Cuyo Group (Figs. 2B, 2C) coincides with the change to a north-northeast trend, whereas southward the same unit is <100 m thick. Taking this into account, we propose that orientations of Andean thrusts and folds were controlled by preexisting normal faults, as observed by Yagupsky et al. (2008) in analog models.

In the eastern part of the study area, a series of basement faults created large anticlines and

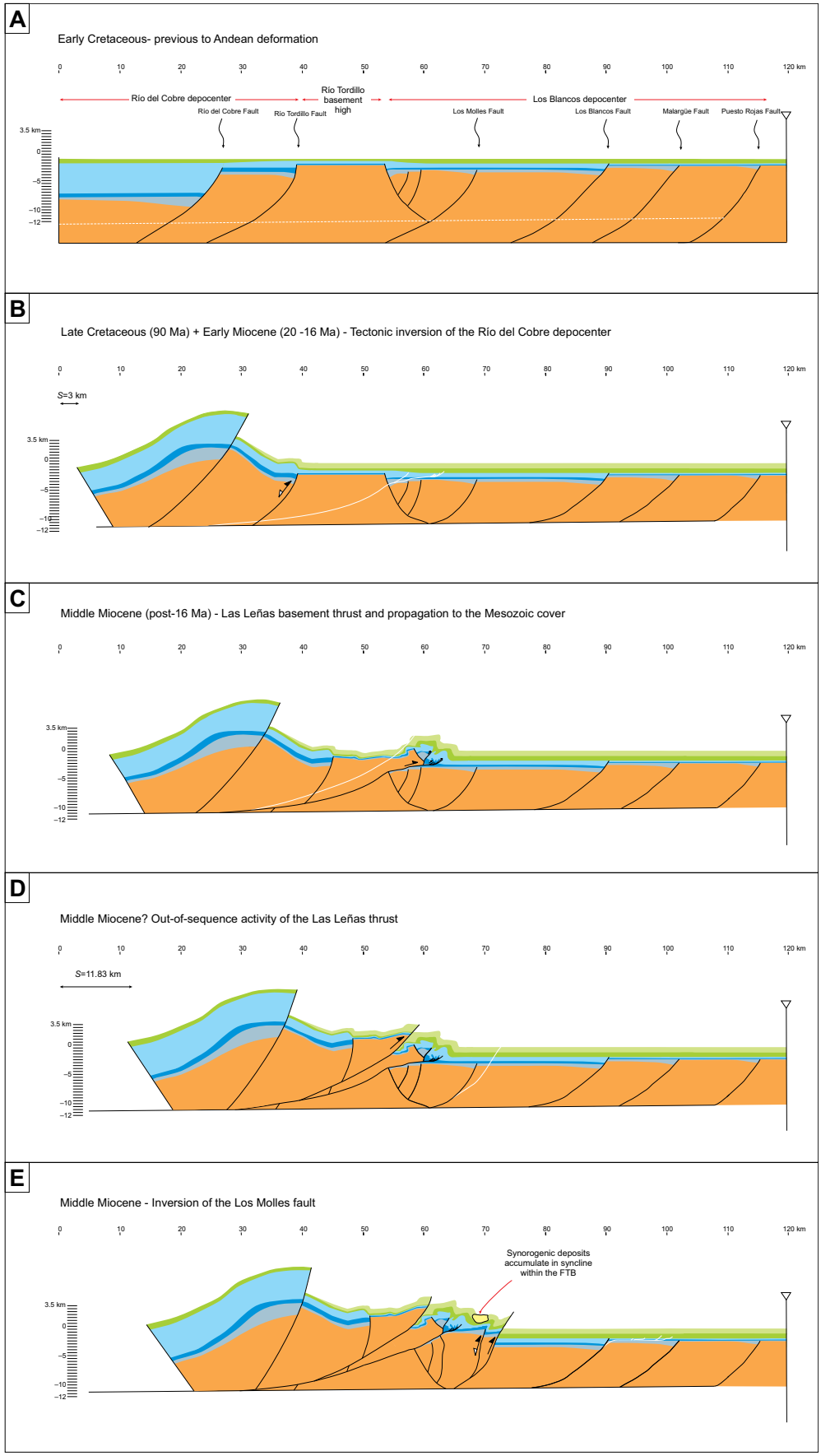

Figure 13 (*on this and following page*). Sequentially restored balanced cross sections of the Malargüe fold-and-thrust belt at 35°S. See Figure 4 for section line. No vertical exaggeration; distances are in kilometers. White lines represent the faults that will form in the following deformation step, except in A, where it represents the main décollement level for the Cenozoic deformation. *S* is shortening calculated for different stages. (A) Geometry of the Neuquén Basin at 35°S in the Cretaceous, prior to Andean compressional deformation. (B) Tectonic inversion of the Río del Cobre depocenter, which took place in two distinct stages in the Late Cretaceous and the early Miocene. The cross section shows the accumulated result of both events. (C) Formation of the Las Leñas basement thrust in the middle Miocene. The basement thrust transfers its displacement to the Mesozoic deposits. (D) Formation of an out-of-sequence fault splay in the Las Leñas thrust. This event could not be dated, and it may be younger than middle Miocene. (E) Inversion of the Los Molles fault, which took place through the reactivation of the main fault and the generation of a shortcut. Note the synorogenic deposits in the syncline. FTB—fold-and-thrust belt.

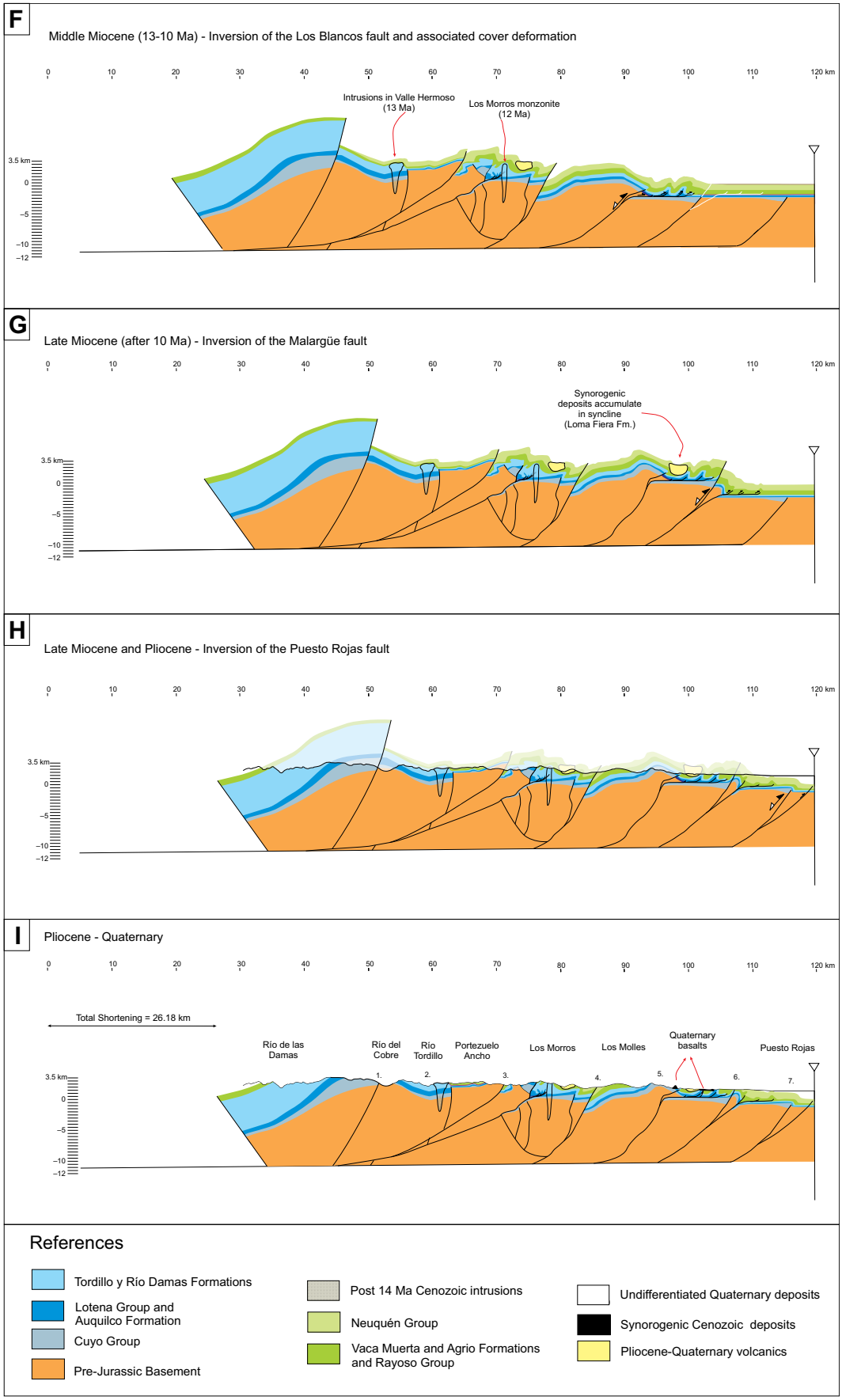

Figure 13 (*continued*). (F) Inversion of the Los Blancos fault, and propagation of the fault to the cover through the décollement level of the Auquilco Formation. Note the emplacement of post-tectonic intrusions at this stage. (G) Late Miocene inversion of the Malargüe fault. (H) Late Miocene and Pliocene inversion of the Puesto Rojas fault. (I) Present state. Numbers 1–7 indicate the main structures as given in Figure 4.

transferred shortening to the cover with detachment levels in the Auquilco and Vaca Muerta Formations (Figs. 13E–13G), leading to the formation of tight folds of <1 km wavelengths. The main structure is the Los Blancos anticline, a symmetric structure with a wavelength of 4 km (Fig. 13F). The easternmost structures of the fold-and-thrust belt at the studied latitude are the Malargüe and Puesto Rojas basement faults (Figs. 13G, 13H), documented from subsurface data (Manceda and Figueroa, 1995; Giampaoli et al., 2002). We interpret these faults as inverted Mesozoic normal faults (see the Discussion for alternative interpretations and implications of the different structural models).

SHORTENING AND SHORTENING RATES

We obtained a shortening of 26.2 km for the Malargüe fold-and-thrust belt, which represents the 22% of the initial length (Fig. 13). As Judge and Allmendinger (2011) pointed out, it is important to determine the uncertainty in shortening obtained from cross sections before using those values as data for geologic models; however, this is not an easy task. Different sources of error include depth to detachment, shape of the deformed wedge, stratigraphic thickness of units, eroded hanging-wall cutoffs, and deformation by minor structures not accounted for in the section (Allmendinger and Judge, 2013). Using the method proposed and the software developed by Judge and Allmendinger (2011), we have attempted to estimate the error in shortening. If we consider that depth to basal fold-and-thrust belt detachment and eroded hanging wall rocks have low uncertainty (<100 m), the Gaussian error is ~3 km (see the Supplemental File [see footnote 1]). Increasing the uncertainty of these parameters increases the error, and for an uncertainty in depth to detachment of 2 km, the shortening and Gaussian error is 26.2 ± 18.6 km, rendering the estimation useless. Because we have used consistent and independent (structural and geophysical) estimations for depth to detachment, we consider that the uncertainty is low and the error is closer to ±3 km.

Accepting the shortening estimations obtained from the cross section, shortening in the inner sector of the belt, where deformation took place between 20 and 16 Ma, reaches 3 km, giving a mean deformation rate of 0.75 mm/yr. The outer sector, with 23.2 km of shortening, was deformed since 16 Ma, giving a rate of 1.45 mm/yr. However, these estimates of deformation rates have significant uncertainties given the limited constraints on deformation ages and uncertainty in shortening.

DISCUSSION

Proposed Structural Models for the Cross Section

In this work we present the first structural model for the inner sector of the Malargüe fold-and-thrust belt at 35°S. The model is based on surface data and geophysical interpretations. The existence of a depocenter of the Neuquén Basin in this area, here named Río del Cobre depocenter, was previously documented (e.g., Gerth, 1931; Legarreta and Uliana, 1999). We propose that Andean deformation took place through the inversion of the normal faults of this depocenter, based on a number of observations (Mescua and Giambiagi, 2012; see Structural Model and Balanced Cross Section discussion).

Previous cross sections for the central and eastern sectors of the study area by Kozlowski et al. (1993) show 35 km of shortening, whereas our estimated shortening is 23.2 km. The difference results from the interpretation of the Los Blancos fault, which in our model is an inverted Mesozoic normal fault, whereas in the Kozlowski et al. (1993) model it is a low-angle basement thrust. A previous section by Manceda and Figueroa (1995), using a higher angle Los Blancos fault controlled by the bounding structure of a half-graben, showed 27 km of estimated shortening. The Giampaoli et al. (2002) cross section also shows the Los Blancos fault as an inverted fault.

A Late Triassic–Early Jurassic extensional depocenter in the middle and eastern sectors of the belt at 35°S was shown previously (Kozlowski et al., 1993; Manceda and Figueroa, 1995; Giampaoli et al., 2002). The Cuyo Group crops out extensively 20 km to the south, in the La Valenciana area (Manceda and Figueroa, 1995). In the study area, Cuyo strata are found in the core of the Los Blancos anticline, which is interpreted to represent the northern termination of the Valenciana depocenter, characterized by a decrease in displacement of the normal faults and thickness of synrift deposits, and at present by a north-south belt of anticlines (Fig. 14). The discontinuous geometry of these anticlines is best explained as resulting from the inversion of segments of normal faults. Trends of the anticlines follow trends of the master faults of the Jurassic rifts (Manceda and Figueroa, 1995): north-northeast in the Valenciana area and north-south in the Los Blancos area, a feature that continues to the north in the Atuel area, where the structures have a north-northwest trend (Bechis et al., 2010). Andean thrusts could also be controlled by the preexisting normal faults, but we favor our interpretation for the Los Blancos fault because of the high potential for inversion of north-south faults in the Andean stress field (Mescua and Giambiagi, 2012). Models using low-angle thrusts for these basement structures imply higher amounts of shortening (Kozlowski et al., 1993) and do not take into account the Mesozoic structures.

For the easternmost Malargüe and Puesto Rojas faults, our structural model is based on relations south of the study area, where deeper levels of basement and Mesozoic synrift units are exposed. In that area, Giambiagi et al. (2009a) interpreted the Malargüe fault as an inverted normal fault with a shortcut fault in its front; in their model, the formation of the structure took place in two episodes: the shortcut fault was generated first, and the inversion of the Mesozoic normal fault took place later (see Giambiagi et al., 2009a for a discussion on the development of this structure). We used the same model for our study area, where the northward plunge of the structure leads to the outcrop of younger (Late Jurassic to Cretaceous) units.

Comparing Shortening Derived from Balanced Cross Sections and Crustal Thickness Estimates

Isacks (1988) presented a methodology to estimate crustal shortening in the Central Andes from cross-sectional crustal area. The calculation is based on area conservation before and after shortening, assuming a constant crustal thickness (T_0) before shortening, tectonic shortening as the only process that leads to crustal thickening, and no erosion (Fig. 15A). Introcaso et al. (1992) calculated a shortening value of S = 90 km at 35°S, using a crustal model built from a gravimetric profile and assuming T_0 = 33. We calculated crustal shortening with the same method using the crustal model of Tassara and Echaurren (2012), which is based on a more extensive and precise compilation of geophysical data. The main uncertainty in this calculation is due to the lack of constrains for the value of T_0. In addition, if magmatic additions contributed to crustal thickening, then tectonic shortening will be overestimated. Although crustal thickening in the Andes was achieved mainly through tectonic shortening, magmatic additions may provide a secondary contribution (Schmitz, 1994; Haschke et al., 2002). Different calculations carried out for the Central Andes have given variable results, with estimated magmatic additions ranging from 1.5% (Francis and Hawkesworth, 1994) to 20% (Schmitz, 1994). Some have proposed a model in which processes of crustal thickening in the Central Andes vary spatially, with tectonic shortening in the eastern part and magmatic additions in the western part (Kono et al., 1989; Sempere and Jacay, 2008). In our case study, considering

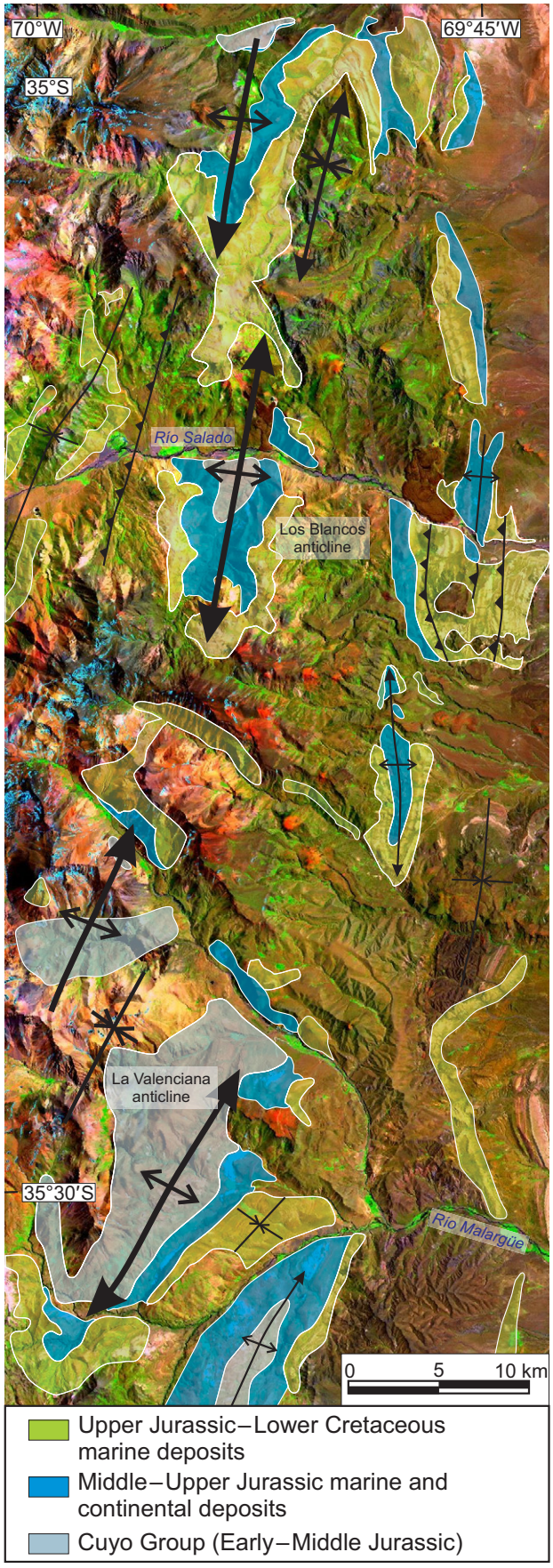

Figure 14. Belt of anticlines interpreted in this work as the result of the inversion of Mesozoic half-grabens. Folds follow the orientations of the main normal faults of the Neuquén Basin.

magmatic additions does not significantly affect shortening amounts (see the calculations presented in the Supplemental File [see footnote 1]). In the following we present our results without considering that magmatic additions contributed to crustal thickening.

Bulk crustal shortening obtained by the calculation also includes shortening in the western slope of the Andes, for which estimates at these latitudes are scarce. At 33.8°S, 150 km to the north of the study area, Farías et al. (2010) estimated shortening of 16 km and 58 km for the western and eastern slopes, respectively. Using the same proportion for our study area gives a shortening of ~8 km for the western slope and 26 km shortening for the eastern slope. As a result of these uncertainties, our calculations can be taken only as a rough approximation of the crustal shortening.

Given uncertainties in T_0, we proceeded to calculate the shortening at 35°S for different T_0 values between 35 and 42 km (Fig. 15B). For values $T_0 < 37$, calculated shortening is $S >$ 70 km. These values, as well as values from Introcaso et al. (1992), are high compared to shortening obtained from cross-section balancing throughout the Malargüe fold-and-thrust belt (Kozlowski et al., 1993; Manceda and Figueroa, 1995; Giambiagi et al., 2009a, 2012, and many others). Shortening values consistent with cross sections are obtained with higher values of initial crustal thickness, such as S = 27.9 km for T_0 = 40 km. This value of T_0 is similar to the global weighted average crustal thickness obtained from a compilation of 560 seismic surveys (Christensen and Mooney, 1995) and suggests that prior to Andean shortening, the crust at 35°S had not been significantly thinned by the Mesozoic extension. This seems to conflict with the repeated marine transgressions that took place during the Mesozoic in the Neuquén Basin, including widespread flooding in Tithonian time (represented by the Vaca Muerta and Baños del Flaco Formations; Fig. 2), likely driven by thermal subsidence after an extensional episode. At present, areas of flooded continental crust have typical thicknesses between 30 and 35 km (Mooney et al., 1998) that, combined with documented extensional structures, suggests that T_0 was less for the Neuquén Basin.

Three possible scenarios are considered.

1. The crust was initially <35 km thick and there is ~60 km of undetected shortening accommodated by eroded or buried structures, which seems unlikely. Furthermore, such a high shortening value would constitute an anomalous value at the regional scale (see the following).

2. The crust had a higher than normal density through basal underplating of mafic magmas during the Triassic (Choiyoi Group) extension,

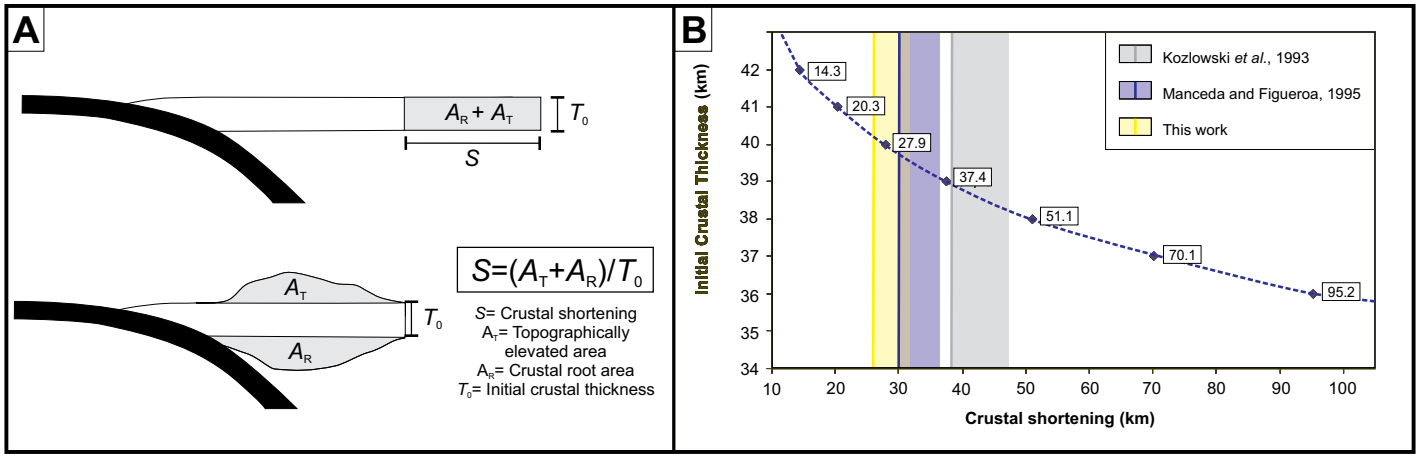

Figure 15. (A) Scheme showing the method for calculating shortening from crustal thickness (following Isacks, 1988). (B) Plot of initial crustal thickness versus shortening for the cross section at 35°S using the crustal model of Tassara and Echaurren (2012). Color lines correspond to the shortening obtained through cross-section balancing by different authors; shaded areas show the addition of 20% of the shortening to include the Chilean sector.

as suggested by Kay et al. (1989) and Llambías et al. (1993); this would have led to a lower elevation of the basin floor and permitted the Mesozoic marine transgressions for T_0 ~ 40 km. However, geophysical studies do not show significant crustal density anomalies in this sector of the Andes (Gilbert et al., 2006; Tassara and Echaurren, 2012).

3. Initial crustal thickness varied across the area due to prior late Paleozoic contraction and Mesozoic extension. We favor this explanation.

Lateral variations in crustal thickness, i.e., a thinner crust below the Neuquén Basin and a thicker crust elsewhere, may account for the average value of crustal thickness obtained in the calculation (Fig. 16). In this respect, the late Paleozoic San Rafael orogeny was responsible for important crustal thickening in the region, and geochemistry of Carboniferous to Permian igneous rocks indicates that the crust was locally >35 km thick as a result of this orogenic event (Mpodozis and Kay, 1990, 1992; Martínez and Giambiagi, 2010). While the crust in the eastern slope of the Andes was stretched during the late Permian and Mesozoic, evidence for crustal thinning to the west is lacking. Farther west, Mesozoic marine beds of intra-arc basins crop out west of Curicó, Chile; this indicates that the crust was not thickened west of this locality. Therefore, a block of thick crust was likely located between the western margin of the Neuquén Basin and the intra-arc basins. A schematic model of crust thickness prior to Andean shortening is shown in Figure 16. In the western sector, in which the Mesozoic intra-arc basins of Chile were developed, the crust thickened gradually from 25 km to ~40 km. To the east, a block of thick crust inherited from the San Rafael orogeny reached a maximum thickness of 45 km. Farther east, the crust of the Neuquén Basin was 32 km thick. The area of this crustal configuration is equivalent to a crust of constant thickness T_0 = 39 km. The block of thick crust underwent early shortening during the Late Cretaceous (Mescua et al., 2013), stretching during the Paleogene development of the Abanico extensional basin (Charrier et al., 2002), and final shortening and uplift during Miocene orogenesis that formed the present Andes. The total amount of shortening in this block obtained from crustal area balancing is ~15–20 km (comparing with the expected 8 km if the proportion was the same than at 33.8°S, see above) suggesting that the proportion of shortening in the western slope increases to the south. Added to the 26 km of shortening in the Neuquén Basin sector obtained from the cross section presented here, these values give 40–45 km of shortening, consistent with the value derived from the calculation based in the Isacks (1988) method with average T_0 = 38–39 km.

Latitudinal Variation in Shortening Derived from Balanced Cross Sections and Crustal Thickness

In order to further test structural models for the study area, we compared latitudinal variations of shortening from balanced cross sections (built by Giambiagi et al., 2012) for the eastern slope of the Andes between 33°30′S and 36°S with variations in crustal thickness and crustal root area obtained from Tassara and Echaurren (2012). Crustal thickness decreases overall southward and has a local minimum at latitudes 34°30′ to 35°S (Figs. 17A and 17B). Variations in maximum crustal thickness and crustal root area (i.e., crustal area below 40 km) and the horizontal shortening from the balanced cross sections (Giambiagi et al., 2012, and this work) display similar patterns. Assuming that crustal thickening took place mainly through tectonic shortening, we would expect a similar variation for the three parameters.

In Figure 17B, different shortening values for the middle and outer sector of the Malargüe fold-and-thrust belt at 35°S are shown: 23.2 km (this work), 27 km (Manceda and Figueroa, 1995), and 35 km (Kozlowski et al., 1993). The inner sector has an estimated 3 km shortening value for a tectonic inversion model (other structural models would give higher shortening in this sector), which must be added to these estimations. A value of S = 35 km (or S = 38 km including the inner sector) results in a pronounced peak in the shortening curve, whereas the curve of maximum crustal thickness lacks a distinct peak. Furthermore, a value of S = 35 km would interrupt the southward decrease in shortening in the Cordillera Principal (curve A in Fig. 17B). Shortening values in the order of 26–30 km for the eastern slope of the Andes at 35°S are more consistent with the regional trends of shortening and crustal thickness. Therefore, a model in which inversion of Mesozoic normal faults and localization of new thrusts played an important role in Andean deformation appears appropriate for the study area.

Implications for Andean Mountain Building

A tectonic model was proposed in which Andean evolution is characterized by alternating phases of contractional and extensional defor-

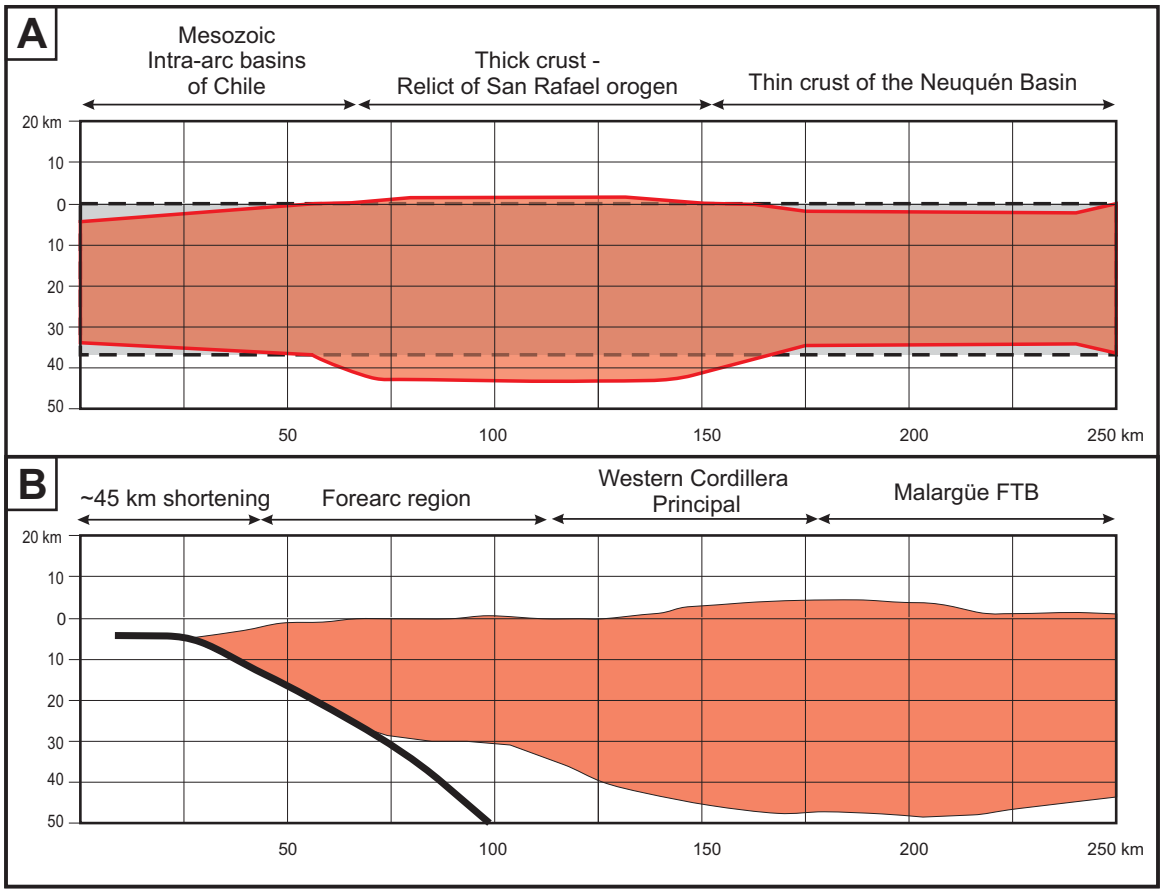

Figure 16. (A) Possible crustal configuration before the beginning of Andean shortening, equivalent to crustal thickness, T_0 = 39 km. (B) Present crustal cross section from the data of Tassara and Echaurren (2012). Note that the Malargüe fold-and-thrust belt (FTB) developed in sector of thin crust corresponding to the Neuquén Basin, with 25 km of shortening, and Western Cordillera Principal developed in block of thicker crust (relict of San Rafael orogeny), with 15 km of shortening.

mation associated with expansion and retraction of the magmatic arc, resulting from variations in the angle of subduction (Ramos and Kay, 2006; Ramos and Folguera, 2010; Folguera and Ramos, 2011). Application of this model led Folguera et al. (2006) to propose that the Andes have been collapsing since Pliocene time at latitudes close to the study area, leading to the development of extensional troughs controlled by normal faults. Folguera et al. (2006) proposed that a north-northwest–trending trough, denominated Las Loicas trough, reached the western sector of the study area. Farías et al. (2009), however, presented evidence of Quaternary thrusting in this sector, and we have not observed any important normal faults during our field work. Instead, contractional deformation migrated steadily toward the east until the Pleistocene, with local out-of-sequence reactivations. Our results indicate that if the model of changes in subduction angle is correct, its structural effects are only developed farther east in the San Rafael block (Fig. 1).

The Cenozoic deformation of the Malargüe fold-and-thrust belt, which is interpreted to have a basal detachment at depths of ~10–12 km, can be explained qualitatively using the critical wedge theory (Davis et al., 1983; Dahlen et al., 1984). In this framework, continued advance of deformation toward the foreland is expected. In the first stages of Andean deformation and uplift, between 20 and 16 Ma, the deformation was localized along the Río del Cobre fault. The long-lived activity of this structure, which was also active during the Late Cretaceous to Paleocene, indicates that it corresponds to a zone of upper crustal weakness. During initial Miocene uplift at 35°S, continued activity of this structure generated a north-northeast–trending uplift estimated oblique to the regional maximum horizontal stress (S_{H_1}) direction, which has varied between 76° and 83° since 26 Ma (Somoza, 1998; Somoza and Ghidella, 2005). Measurements of 325 subvertical volcanic dikes (dated as 16 Ma; Ar/Ar total rock ages of 16.3 ± 0.1 and 16.1 ± 0.2 Ma; Sruoga et al., 2008) located in the Cerros Matancilla, immediately east of the Río del Cobre fault (Fig. 18), indicates that at that time, the local S_{H_1} was oriented east-southeast (Mescua et al., 2009). An alternative to this would be a postemplacement rotation of the dikes about a vertical axis, although the limited paleomagnetic work carried out in the region suggests that such rotations did not occur (Iglesia Llanos et al., 2008). We propose that this local stress rotation is the result of the topographic effect of the north-northeast–trending range formed after 4 m.y. of activity of the Río del Cobre fault between 20 and 16 Ma. The dike-in-dike structure observed in that locality (Fig. 18A) led Sruoga et al. (2008) to invoke local extensional conditions to allow the intrusion of the successive dikes. Local extension or transcurrence within the regional compressional stress field can be related to uplift concentrated in the range west of the Río del Cobre fault that could have taken

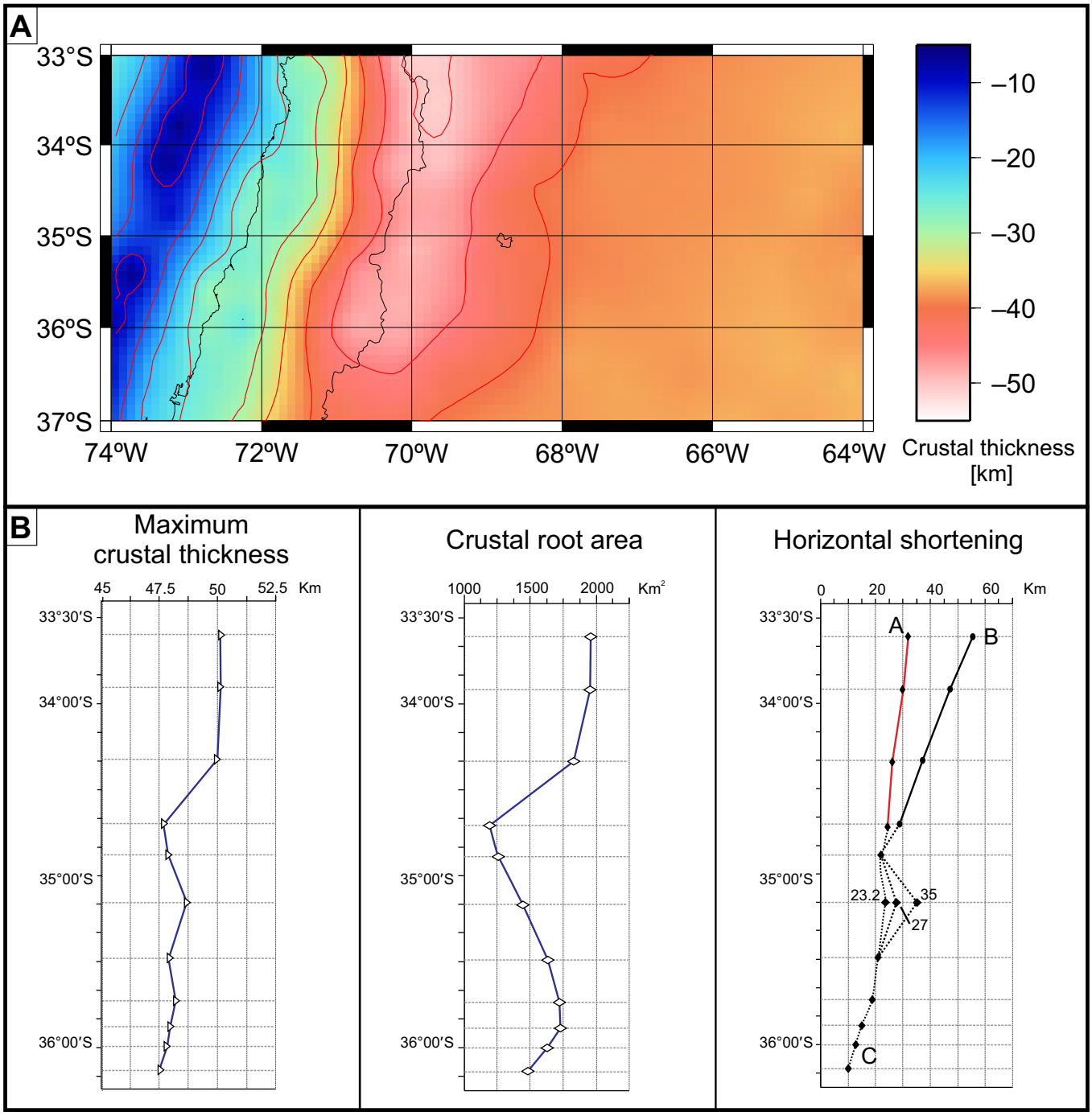

Figure 17. (A) Crustal thickness in the Andean margin between 33° and 37°S (from Tassara and Echaurren, 2012). (B) Variation with latitude of maximum crustal thickness and crustal root area from the crustal model, and horizontal shortening from balanced cross sections for the central and eastern Malargüe fold-and-thrust belt (MFTB). Black curve includes frontal Cordillera Frontal and Aconcagua and Malargüe fold-and-thrust belts, whereas red curve is for the fold-and-thrust belts only.

the orogenic wedge locally to a supercritical state, leading the maximum stress to the vertical position (Molnar and Lyon-Caen, 1988), and triggering local orogen-parallel extension. This effect may have been also aided by the decrease in convergence velocity and coupling between the Nazca and South American plates at that time (Somoza and Ghidella, 2005).

Advance of the deformation to east, prevented previously by the competent Las Leñas basement block, eventually took place with the formation of the Las Leñas thrust. Further advance to the east was favored by preexisting structures which were inverted, like the Los Blancos fault. During this advance to the east, out-of-sequence deformation along the El Fierro and Las Leñas thrusts helped to maintain taper of the deforming wedge and allow the propaga-

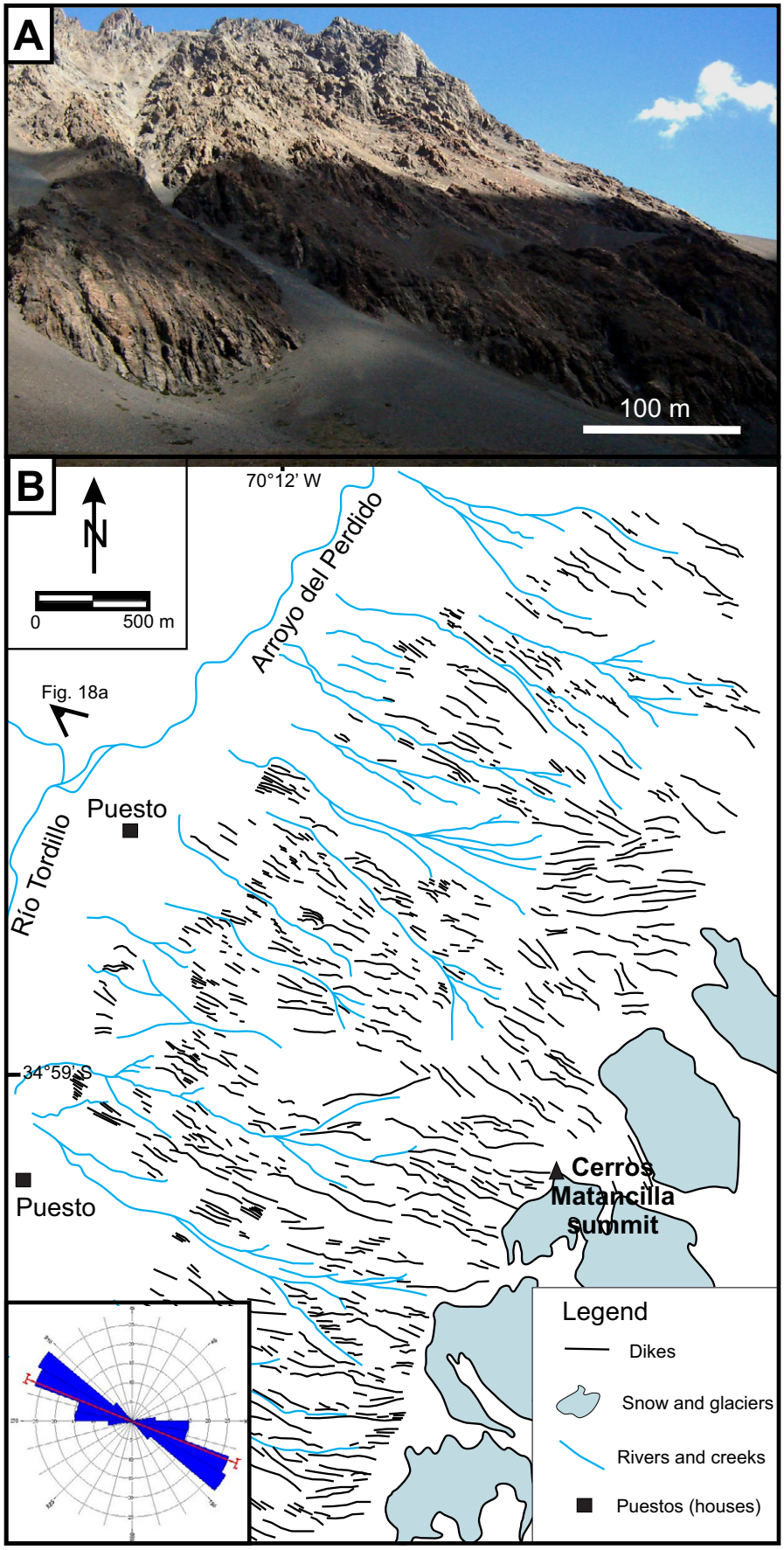

Figure 18. (A) Field photograph of the subvertical dikes of the Cerros Matancilla. See Figure 4 for location. (B) Mapped dikes in the Cerros Matancilla. Rose diagram shows the orientation distribution; mean-parallels the S_{H_1} (maximum horizontal stress direction).

tion of the deformation toward the foreland. A more precise determination of the age of out-of-sequence activity of these structures is required in order to evaluate their activity as a result of critical wedge dynamics.

CONCLUSIONS

A new structural model has been developed for Andean deformation at 35°S, a model in which the basement structures correspond to both inverted Mesozoic normal faults and new thrusts. Faults interpreted as inverted structures, including the Río del Cobre, Tordillo, and Los Blancos faults, are high-angle reverse faults, across which thickness and facies of Mesozoic rocks varied. The other major structure in the cross section, the Las Leñas fault, is interpreted as an Andean low-angle thrust. Where faults reached the Mesozoic cover, they followed weak layers in this succession (shales and evaporites) as detachment levels. The rheology and bed thickness of the cover rocks also influenced the deformation style (fold style and wavelength, folding versus thrusting) on a more local scale.

A balanced cross section across the eastern slope of the Andes had an estimated shortening of 26.2 km, smaller than previous estimates based on models that did not incorporate tectonic inversion.

Using a crustal model built from a geophysical database, we calculated crustal shortening for various initial crustal thicknesses. An initial mean crustal thickness of 38–40 km yielded calculated shortening consistent with cross sections. Mesozoic marine deposits of the Neuquén Basin suggest that crust was locally thinner. We propose a crustal model in which the crustal thinning in the Neuquén Basin was compensated by a block of thick crust located to the west, a root relict of the Early Paleozoic San Rafael orogen.

We analyzed the regional trends of shortening and crustal thickness along strike in the segment of the Andes between 33°30′S and 36°S in order to evaluate the proposed structural models. Models that do not take into account the inherited structures predict values of shortening that are too high when comparing the curves of crustal thickness and shortening. In contrast, our

hybrid model based on tectonic inversion and new thrusts fits in a curve of shortening more similar to the curve of crustal thickness, and is therefore more compatible with these data.

Our results underscore the role of upper plate inherited characteristics in subduction orogeny, especially preexisting faults that conformed weakness zones and were inverted during orogenesis.

ACKNOWLEDGMENTS

We thank A.E. Amato for a review of a previous version of this work, and Sean Mulcahy and an anonymous reviewer, whose insightful comments and suggestions allowed us to improve the manuscript significantly. Associate Editor T. Pavlis and Science Editor T. Wawrzyniec provided helpful reviews. We acknowledge funding from Agencia de Promoción Científica y Tecnológica (projects PICT-14144 and PICT-2011-1079) and Consejo Nacional de Investigaciones Científicas y Técnicas (project PIP 5843). We also thank Midland Valley, Inc., for providing an academic license for their software Move. This is a contribution to International Geoscience Programme Project 586Y, Geodynamic Processes in the Andes.

REFERENCES CITED

Allmendinger, R.W., 1998, Inverse and forward modeling of trishear fault-propagation folds: Tectonics, v. 17, p. 640–656, doi:10.1029/98TC01907.

Allmendinger, R.W., and Gubbels, T., 1996, Pure and simple shear plateau uplift: Altiplano–Puna, Argentina and Bolivia: Tectonophysics, v. 259, p. 1–13, doi:10.1016/0040-1951(96)00024-8.

Allmendinger, R., and Judge, P., 2013, Stratigraphic uncertainty and errors in shortening from balanced sections in the North American Cordillera: Geological Society of America Bulletin, v. 125, p. 1569–1579, doi:10.1130/B30871.1.

Allmendinger, R.W., Ramos, V.A., Jordan, T.E., Palma, M., and Isacks, B.L., 1983, Paleogeography and Andean structural geometry, northwest Argentina: Tectonics, v. 2, p. 1–16, doi:10.1029/TC002i001p00001.

Allmendinger, R.W., Zapata, T., Manceda, R., and Dzelalija, F., 2004, Trishear kinematic modeling of structures, with examples from the Neuquén Basin, Argentina, *in* McClay, K.R., ed., Thrust tectonics and hydrocarbon systems: American Association of Petroleum Geologists Memoir 82, p. 356–371.

Aparicio, E.P., 1950, Hallazgo de sedimentos paleozoicos en las cabeceras del río Salado: Revista de la Asociación Geológica Argentina, v. 5, no. 3, p. 127–135.

Baldauf, P.E., 1997, Timing of the uplift of the Cordillera Principal, Mendoza Province, Argentina [Ph.D. thesis]: Washington, D.C., George Washington University, 356 p.

Barazangi, M., and Isacks, B.L., 1976, Spatial distribution of earthquakes and subduction of the Nazca plate beneath South America: Geology, v. 4, p. 686–692, doi:10.1130/0091-7613(1976)4<686:SDOEAS>2.0.CO;2.

Barbosa, V.C.F., Silva, J.B.C., and Medeiros, W.E., 1999, Stability analysis and improvement of structural index estimation in Euler deconvolution: Geophysics, v. 64, p. 48–60, doi:10.1190/1.1444529.

Bechis, F., Giambiagi, L.B., Garcia, V., Lanes, S., Cristallini, E., and Tunik, M., 2010, Kinematic analysis of a transtensional fault system: The Atuel depocenter of the Neuquén basin, southern Central Andes, Argentina: Journal of Structural Geology, v. 32, p. 886–899, doi:10.1016/j.jsg.2010.03.009.

Burckhardt, C., 1900, Profils geoloqiques transversaux de la Cordillere Argentino-Chilienne. Stratigraphie et Tectonique: Anales del Museo de La Plata, Sección Geología y Minería, tomo 2, 136 p.

Cegarra, M.I., and Ramos, V.A., 1996, La faja plegada y corrida del Aconcagua, *in* Ramos, V.A., ed., Geología de la región del Aconcagua, provincias de San Juan y Mendoza: Dirección Nacional del Servicio Geológico, Subsecretaria de Minería de la Nación, Anales, v. 24, p. 387–422.

Charrier, R., 1979, El Triásico de Chile y regiones adyacentes de Argentina: Una reconstrucción paleogeográfica y paleoclimática: Comunicaciones, v. 26, p. 1–37.

Charrier, R., Wyss, A.R., Flynn, J.J., Swisher, C., Norell, M.A., Zapata, F., McKenna, M.C., and Novacek, M.J., 1996, New evidence for late Mesozoic–early Cenozoic evolution of the Chilean Andes in the Upper Tinguiririca Valley (35°S), central Chile: Journal of South American Earth Sciences, v. 9, p. 393–422, doi:10.1016/S0895-9811(96)00035-1.

Charrier, R., Baeza, O., Elgueta, S., Flynn, J.J., Gans, P., Kay, S.M., Muñoz, N., Wyss, A.R., and Zurita, E., 2002, Evidence for Cenozoic extensional basin development and tectonic inversion south of the flat-slab segment, southern Central Andes, Chile (33°–36°S): Journal of South American Earth Sciences, v. 15, p. 117–139, doi:10.1016/S0895-9811(02)00009-3.

Charrier, R., Pinto, L., and Rodríguez, M.P., 2007, Tectonostratigraphic evolution, *in* Moreno, T., and Gibbons, W., eds., The Geology of Chile: The Geological Society, London, p. 21–114.

Christensen, N.I., and Mooney, W.D., 1995, Seismic velocity structure and composition of the continental crust: A global view: Journal of Geophysical Research, v. 100, no. B7, p. 9761–9788, doi:10.1029/95JB00259.

Combina, A., and Nullo, F., 2000, La Formación Loma Fiera (Mioceno superior) y su relación con el volcanismo y el tectonismo neógeno, Mendoza: Revista de la Asociación Geológica Argentina, v. 55, no. 3, p. 201–210.

Cooper, G.R.J., 2006, Obtaining dip and susceptibility information from Euler deconvolution using the Hough transform: Computers & Geosciences, v. 32, p. 1592–1599, doi:10.1016/j.cageo.2006.02.019.

Currie, J.B., Patnode, H.W., and Trump, R.P., 1962, Development of folds in sedimentary strata: Geological Society of America Bulletin, v. 73, p. 655–674, doi:10.1130/0016-7606(1962)73[655:DOFISS]2.0.CO;2.

Davis, D., Suppe, J., and Dahlen, F.A., 1983, Mechanics of fold-and-thrust belts and accretionary wedges: Journal of Geophysical Research, v. 88, no. B2, p. 1153–1178, doi:10.1029/JB088iB02p01153.

Dahlen, F.A., Suppe, J., and Davis, D., 1984, Mechanics of fold-and-thrust belts and accretionary wedges: cohesive Coulomb theory: Journal of Geophysical Research, v. 89, no. B12, p. 10087–10101, doi:10.1029/JB089iB12p10087.

Davidson, J., and Vicente, J.C., 1973, Características paleogeográficas y estructurales del área fronteriza de las nacientes del Teno (Chile) y Santa Elena (Argentina) (Cordillera Principal, 35° a 35° 15′ latitud sur): Congreso Geológico Argentino, 5, Actas, v. 5, p. 11–55.

Di Carlo, D., and Cristallini, E., 2007, Estructura de la margen norte del río Grande, Bardas Blancas, provincia de Mendoza: Revista de la Asociación Geológica Argentina, v. 62, p. 187–199.

Dimieri, L., 1997, Tectonic wedge geometry at Bardas Blancas, Southern Andes (36°S), Argentina: Journal of Structural Geology, v. 19, no. 11, p. 1419–1422, doi:10.1016/S0191-8141(97)00055-2.

Dimieri, L., Di Nardo, L., Frisicale, M., Delpino, S., Fortunatti, N., and Nullo, F., 1997, Inversión tectónica: Un mecanismo ineficiente para producir acortamiento: Congreso Geológico Chileno, 8, Actas, v. I, p. 52–54.

Erslev, E.A., 1991, Trishear fault-propagation folding: Geology, v. 19, p. 617–620, doi:10.1130/0091-7613(1991)019<0617:TFPF>2.3.CO;2.

Farías, M., Tapia, F., and Comte, D., 2009, La falla Calabozos: un cabalgamiento activo en la alta cordillera de Curicó: Congreso Geológico Chileno, 12, Actas, CD S9_23, 3 p.

Farías, M., Comte, D., Charrier, R., Martinod, J., David, C., Tassara, A., Tapia, F., and Fock, A., 2010, Crustal-scale structural architecture in central Chile based on seismicity and surface geology: Implications for Andean mountain building: Tectonics, v. 29, doi:10.1029/2009TC002480.

Folguera, A., and Ramos, V.A., 2011, Repeated eastward shifts of arc magmatism in the Southern Andes: A revision to the long-term pattern of Andean uplift and magmatism: Journal of South American Earth Sciences, v. 32, p. 531–546, doi:10.1016/j.jsames.2011.04.003.

Folguera, A., Zapata, T., and Ramos, V.A., 2006, Late Cenozoic extension and the evolution of the Neuquén Andes, *in* Kay, S.M., and Ramos, V.A., eds., Evolution of an Andean margin: A tectonic and magmatic view from the Andes to the Neuquén Basin (35°–39°S lat): Geological Society of America Special Paper 407, p. 267–285, doi:10.1130/2006.2407(12).

Francis, P.W., and Hawkesworth, C.J., 1994, Late Cenozoic rates of magmatic activity in the Central Andes and their relationships to continental crust formation and thickening: Geological Society of London Journal, v. 151, p. 845–854, doi:10.1144/gsjgs.151.5.0845.

Gansser, A., 1973, Facts and theories on the Andes: Geological Society of London Journal, v. 129, p. 93–131, doi:10.1144/gsjgs.129.2.0093.

Gerth, E., 1931, La estructura geológica de la Cordillera argentina entre el río Grande y río Diamante en el sur de la provincia de Mendoza: Academia Nacional de Ciencias, Actas, v. 10, p. 125–172.

Giambiagi, L.B., Alvarez, P., Godoy, E., and Ramos, V.A., 2003, The control of preexisting extensional structures on the evolution of the southern sector of the Aconcagua fold and thrust belt, southern Andes: Tectonophysics, v. 369, p. 1–19, doi:10.1016/S0040-1951(03)00171-9.

Giambiagi, L.B., Alvarez, P.P., Bechis, F., and Tunik, M., 2005, Influencia de las estructuras de rift triásicas–jurásicas sobre el estilo de deformación en las fajas plegadas y corridas Aconcagua y Malargüe: Revista de la Asociación Geológica Argentina, v. 60, p. 661–671.

Giambiagi, L.B., Bechis, F., García, V., and Clark, A., 2008, Temporal and spatial relationship between thick- and thin-skinned deformation in the Malargüe fold and thrust belt, southern Central Andes: Tectonophysics, v. 459, p. 123–139, doi:10.1016/j.tecto.2007.11.069.

Giambiagi, L., Ghiglione, M., Cristallini, E., and Bottesi, G., 2009a, Kinematic models of basement/cover interactions: Insights from the Malargüe fold and thrust belt, Mendoza, Argentina: Journal of Structural Geology, v. 31, p. 1443–1457, doi:10.1016/j.jsg.2009.10.006.

Giambiagi, L.B., Tunik, M., Barredo, S., Bechis, F., Ghiglione, M., Alvarez, P., and Drosina, M., 2009b, Cinemática de apertura del sector norte de la cuenca Neuquina: Revista de la Asociación Geológica Argentina, v. 65, no. 1, p. 140–153.

Giambiagi, L.B., Mescua, J.F., Bechis, F., Tassara, A., and Hoke, G., 2012, Thrust belts of the southern Central Andes: Along-strike variations in shortening, topography, crustal geometry and denudation: Geological Society of America Bulletin, v. 124, p. 1339–1351, doi:10.1130/B30609.1.

Giampaoli, P., Dajczgewand, D., and Dzelalija, F., 2002, La estructura del sector externo de la faja plegada y corrida de Malargüe a la latitud del río Salado, cuenca neuquina surmendocina, Argentina: Congreso Geologico Argentino, 15, Actas, v. 3, p. 168–173.

Gilbert, H., Beck, S., and Zandt, G., 2006, Lithospheric and upper mantle structure of central Chile and Argentina: Geophysical Journal International, v. 165, p. 383–398, doi:10.1111/j.1365-246X.2006.02867.x.

Godoy, E., Yáñez, G., and Vera, E., 1999, Inversion of an Oligocene volcano-tectonic basin and uplifting of its superimposed Miocene magmatic arc in the Chilean Central Andes: First seismic and gravity evidences: Tectonophysics, v. 306, p. 217–236, doi:10.1016/S0040-1951(99)00046-3.

Gulisano, C.A., 1981, El Ciclo Cuyano en el norte de Neuquén y sur de Mendoza: Congreso Geológico Argentino, 8, Actas, v. 3, p. 579–592.

Haschke, M., Siebel, W., Gunther, A., and Scheuber, E., 2002, Repeated crustal thickening and recycling during the Andean orogeny in north Chile (21–26°S): Journal of Geophysical Research, v. 107, no. B1, doi:10.1029/2001JB000328.

Hayward, A.B., and Graham, R.H., 1989, Some geometrical characteristics of inversion, *in* Cooper, M.A., and Williams, G.D., eds., Inversion tectonics: Geological

Society of London Special Publication 44, p. 17–39, doi:10.1144/GSL.SP.1989.044.01.03.

Iglesia Llanos, P., Riccardi, A.C., and Singer, S.E., 2008, A comment on Early Jurassic paleomagnetic study of Lower Jurassic marine strata from the Neuquén basin, Argentina: A new Jurassic apparent polar wander path for South America: Reply: Earth and Planetary Science Letters, v. 265, p. 316–319, doi:10.1016/j.epsl.2007.10.020.

Introcaso, A., Pacino, M.C., and Fraga, H., 1992, Gravity, isostasy and Andean crustal shortening between latitudes 30 and 35°S: Tectonophysics, v. 205, p. 31–48, doi:10.1016/0040-1951(92)90416-4.

Isacks, B.L., 1988, Uplift of the Central Andean Plateau and bending of the Bolivian orocline: Journal of Geophysical Research, v. 93, no. B4, p. 3211–3231, doi:10.1029/JB093iB04p03211.

Jarrard, R.D., 1986, Relations among subduction parameters: Reviews in Geophysics, v. 42, p. 217–284, doi:10.1029/RG024i002p00217.

Jordan, T., Isacks, B., Allmendinger, R.W., Brewer, J.A., Ramos, V.A., and Ando, C.J., 1983, Andean tectonics related to geometry of subducted Nazca plate: Geological Society of America Bulletin, v. 94, p. 341–361, doi:10.1130/0016-7606(1983)94<341:ATRTGO>2.0.CO;2.

Judge, P., and Allmendinger, R., 2011, Assessing uncertainties in balanced cross-sections: Journal of Structural Geology, v. 33, p. 458–467, doi:10.1016/j.jsg.2011.01.006.

Kay, S.M., Ramos, V.A., Mpodozis, C., and Sruoga, P., 1989, Late Paleozoic to Jurassic silicic magmatism at the Gondwana margin: Analogy to the Middle Proterozoic in North America?: Geology, v. 17, p. 324–328, doi:10.1130/0091-7613(1989)017<0324:LPTJSM>2.3.CO;2.

Kley, J., Monaldi, C.R., and Saltify, J.A., 1999, Along-strike segmentation of the Andean foreland: Causes and consequences: Tectonophysics, v. 301, p. 75–94, doi:10.1016/S0040-1951(98)90223-2.

Klohn, C., 1960, Geología de la Cordillera de los Andes de Chile Central, Provincias de Santiago, O'Higgins, Colchagua y Curicó: Investigaciones Geológicas (Chile), Boletín no. 8, 95 p..

Kono, M., Fukao, Y., and Yamamoto, A., 1989, Mountain building in the Central Andes: Journal of Geophysical Research, v. 94, no. B4, p. 3891–3905, doi:10.1029/JB094iB04p03891.

Kozlowski, E., Cruz, C., Rebay, G., and Baldi, J., 1984, Planos geológicos a escala 1:50.000 de cuenca Neuquina, zonas Río Atuel-Río Salado y Río Salado-Río Malargüe: Buenos Aires, Gerencia General de Exploración, Yacimientos Petrolíferos Fiscales (unpublished).

Kozlowski, E., Manceda, R., and Ramos, V.A., 1993, Estructura, *in* Ramos, V.A., ed., Geología y Recursos Naturales de Mendoza: 12 Congreso Geológico Argentino y 2 Congreso de Exploración de Hidrocarburos, Relatorio, p. 235–256.

Lanés, S., 2005, Late Triassic to Early Jurassic sedimentation in northern Neuquén Basin, Argentina: Tectosedimentary evolution of the first transgression: Geologica Acta, v. 3, no. 2, p. 81–106.

Lanés, S., Giambiagi, L., Bechis, F., and Tunik, M., 2008, Late Triassic–Early Jurassic successions from the Atuel depocenter: Depositional systems, sequence stratigraphy and tectonic controls: Revista de la Asociación Geológica Argentina, v. 63, p. 534–548.

Legarreta, L., and Kozlowski, E., 1984, Secciones condensadas del Jurásico-Cretácico de los Andes del sur de Mendoza: estratigrafía y significado tectosedimentario: Congreso Geológico Argentino, 9, Actas, v. 1, p. 286–297.

Legarreta, L., and Uliana, M.A., 1996, The Jurassic succession in west-central Argentina: Stratal patterns, sequences and paleogeographic evolution: Palaeogeography, Palaeoclimatology, Palaeoecology, v. 120, p. 303–330, doi:10.1016/0031-0182(95)00042-9.

Legarreta, L., and Uliana, M.A., 1999, El Jurásico y Cretácico de la Cordillera Principal y la cuenca Neuquina. 1. Facies sedimentarias, *in* Caminos, R., ed., Geología Argentina: Servicio Geológico y Minero Argentino, Instituto de Geología y Recursos Minerales, Anales, v. 29, p. 399–416.

Llambías, E.J., Kleiman, L.E., and Salvarredi, J.A., 1993, El magmatismo gondwánico, *in* Ramos, V.A., ed., Geología y Recursos Naturales de Mendoza: 12 Congreso Geológico Argentino y 2 Congreso de Exploración de Hidrocarburos, Relatorio, p. 53–64.

Manceda, R., and Figueroa, D., 1995, Inversion of the Mesozoic Neuquen rift in the Malargüe fold-thrust belt, Mendoza, Argentina, *in* Tankard, A.J., et al., eds., Petroleum basins of South America: American Association of Petroleum Geologists Memoir 62, p. 369–382.

Marques, F.O., and Nogueira, C.R., 2008, Normal fault inversion by orthogonal compression: Sandbox experiments with weak faults: Journal of Structural Geology, v. 30, p. 761–766, doi:10.1016/j.jsg.2008.02.015.

Martínez, A., and Giambiagi, L., 2010, Evolución petrológica y geoquímica del magmatismo bimodal permo-triásico del Grupo Choiyoi en el Cordón del Portillo, Mendoza, Argentina: Trabajos de Geología, v. 30, p. 432–451.

Mescua, J.F., and Giambiagi, L.B., 2012, Fault inversion vs. new thrust generation: A case study in the Malargüe fold-and-thrust belt, Andes of Argentina: Journal of Structural Geology, v. 35, p. 51–63, doi:10.1016/j.jsg.2011.11.011.

Mescua, J.F., Giambiagi, L.B., and Bechis, F., 2008, Evidencias de tectónica extensional en el Jurásico tardío (Kimeridgiano) del suroeste de la provincia de Mendoza: Revista de la Asociación Geológica Argentina, v. 63, p. 512–519.

Mescua, J.F., Giambiagi, L.B., and Ramos, V.A., 2009, Los diques de los cerros Matancilla: Reflejo del campo de esfuerzos mioceno temprano (16 Ma) en la faja plegada y corrida de Malargüe?: Congreso Geológico Chileno, 12, Actas, CD S9_55, 4 p.

Mescua, J.F., Giambiagi, L., and Ramos, V.A., 2010, Inherited controls in Andean structure in a sector of the Malargüe fold and thrust belt, Mendoza province, Argentina: Trabajos de Geología, v. 30, p. 81–86.

Mescua, J.F., Giambiagi, L.B., and Ramos, V.A., 2013, Late Cretaceous uplift in the Malargüe fold-and-thrust belt (35°S), southern Central Andes of Argentina and Chile: Andean Geology, v. 40, no. 1, p. 102–116, doi:10.5027/andgeoV40n1-a05.

Molnar, P., and Lyon-Caen, H., 1988, Some simple aspects of the support, structure and evolution of mountain belts, *in* Clark, S.D., et al., eds., Processes in continental lithospheric deformation: Geological Society of America Special Paper 218, p. 179–208, doi:10.1130/SPE218-p179.

Mooney, W.D., Laske, G., and Guy Masters, T., 1998, CRUST 5.1: A global crustal model at 5°×5°: Journal of Geophysical Research, v. 103, no. B1, p. 727–747, doi:10.1029/97JB02122.

Mpodozis, C., and Kay, S.M., 1990, Provincias magmáticas ácidas de los Andes Chilenos (28°S-31°S) y evolución tectónica de Gondwana: Revista Geológica de Chile, v. 17, p. 153–180.

Mpodozis, C., and Kay, S.M., 1992, Late Paleozoic to Triassic evolution of the Gondwana margin: Evidence from Chilean Frontal Cordillera batholiths (28°S to 31°S): Geological Society of America Bulletin, v. 104, p. 999–1014, doi:10.1130/0016-7606(1992)104<0999:LPTTEO>2.3.CO;2.

Mushayandebvu, M.F., Lesurz, V., Reid, A.B., and Fairhead, J.D., 2004, Grid Euler deconvolution with constraints for 2D structures: Geophysics, v. 69, p. 489–496, doi:10.1190/1.1707069.

Nieuwland, D.A., Leutscher, J.H., and Gast, J., 2000, Wedge equilibrium in fold-and-thrust belts: Prediction of out-of-sequence thrusting based on sandbox experiments and natural examples: Netherlands Journal of Geosciences, v. 79, no. 1, p. 81–91.

Nullo, F.E., Stephens, G.C., Otamendi, J., and Baldauf, P.E., 2002, El volcanismo del Terciario superior del sur de Mendoza: Revista de la Asociación Geológica Argentina, v. 57, p. 119–132.

Nullo, F.E., Stephens, G.C., Combina, A.M., Dimieri, L., Baldauf, P.E., and Bouza, P., 2005, Hoja Geológica 3569-III Malargüe, Provincia de Mendoza: Instituto de Geología y Recursos Minerales, Servicio Geológico Minero Argentino, Boletín 346, 85 p.

Oncken, O., Hindle, D., Kley, J., Elger, K., Victor, P., and Schemmann, K., 2006, Deformation of the Central Andean upper plate system—Facts, fiction and constraints for plateau models, *in* Oncken, O., et al., eds., The Andes: Active subduction orogeny (Frontiers in Earth Sciences): Berlin, Springer, p. 3–28.

Pángaro, F., Ramos, V.A., and Godoy, E., 1996, La faja plegada y corrida de la Cordillera Principal de Argentina y Chile a la latitud del Cerro Palomares (33°35′S): 13 Congreso Geológico Argentino y 3 Congreso Exploración de Hidrocarburos, Actas, v. 2, p. 315–324.

Pearson, D.M., Kapp, P., DeCelles, P.G., Reiners, P.W., Gehrels, G.E., Ducea, M.N., and Pullen, A., 2013, Influence of Pre-Andean crustal structure on Cenozoic thrust belt kinematics and shortening magnitude: Northwestern Argentina: Geosphere, v. 9, no. 6, doi:10.1130/GES00923.1.

Ramos, V.A., 1999, Plate tectonic setting of the Andean Cordillera: Episodes, v. 22, p. 183–190.

Ramos, V.A., 2010, The tectonic regime along the Andes: Mesozoic and present-day regimes: Geological Journal, v. 45, p. 2–25, doi:10.1002/gj.1193.

Ramos, V.A., and Folguera, A., 2010, Payenia volcanic province in the Southern Andes: An appraisal of an exceptional Quaternary tectonic setting: Journal of Volcanology and Geothermal Research, v. 201, p. 53–64, doi:10.1016/j.jvolgeores.2010.09.008.

Ramos, V.A., and Kay, S.M., 2006, Overview of the tectonic evolution of the southern Central Andes of Mendoza and Neuquén (35°–39°S latitude), *in* Kay, S.M., and Ramos, V.A., eds., Evolution of an Andean margin: A tectonic and magmatic view from the Andes to the Neuquén Basin (35°–39°S lat), Geological Society of America Special Paper 407, p. 1–18, doi:10.1130/2006.2407(01).

Ramos, V.A., Cegarra, M., and Cristallini, E., 1996, Cenozoic tectonics of the High Andes of west-central Argentina: Tectonophysics, v. 259, p. 185–200, doi:10.1016/0040-1951(95)00064-X.

Ramos, V.A., Cristallini, E.O., and Pérez, D.J., 2002, The Pampean flat-slab of the Central Andes: Journal of South American Earth Sciences, v. 15, p. 59–78, doi:10.1016/S0895-9811(02)00006-8.

Ramsay, J.G., 1967, Folding and fracturing of rocks: New York, McGraw-Hill, 568 p.

Reid, A.B., Allsop, J.M., Granser, H., Millett, A.J., and Somerton, I.W., 1990, Magnetic interpretation in three dimensions using Euler deconvolution: Geophysics, v. 55, p. 80–91, doi:10.1190/1.1442774.

Rojas, L., and Radic, J.P., 2002, Estilos de deformación del basamento y de la cobertura sedimentaria en la faja plegada y fallada de Malargüe en el área de Puesto Rojas, Mendoza, Argentina: Congreso Geológico Argentino, 15, Actas, v. 2, p. 224–229.

Roy, L., Agarwal, B.N.P., and Shaw, R.K., 2000, A new concept in Euler deconvolution of isolated gravity anomalies: Geophysical Prospecting, v. 48, p. 559–575, doi:10.1046/j.1365-2478.2000.00203.x.

Schmitz, M., 1994, A balanced model of the southern Central Andes: Tectonics, v. 13, p. 484–492, doi:10.1029/93TC02232.

Sempere, T., and Jacay, J., 2008, Anatomy of the Central Andes: Distinguishing between western, magmatic Andes and eastern, tectonic Andes: International Symposium on Andean Geodynamics (ISAG2008), 7th, extended abstracts, p. 504–507.

Sibson, R.H., 1985, A note on fault reactivation: Journal of Structural Geology, v. 7, p. 751–754, doi:10.1016/0191-8141(85)90150-6.

Silvestro, J., Kraemer, P., Achilli, F., and Brinkworth, W., 2005, Evolución de las cuencas sinorogénicas de la Cordillera Principal entre 35°-36° S, Malargüe: Revista de la Asociación Geológica Argentina, v. 60, p. 627–643.

Sobolev, S.V., and Babeyko, A.Y., 2005, What drives orogeny in the Andes?: Geology, v. 33, p. 617–620, doi:10.1130/G21557.1.

Somoza, R., 1998, Updated Nazca (Farallon)–South America relative motions during the last 40 Ma: Implications for mountain building in the central Andean region: Journal of South American Earth Sciences, v. 11, no. 3, p. 211–215, doi:10.1016/S0895-9811(98)00012-1.

Somoza, R., and Ghidella, M.E., 2005, Convergencia en el margen occidental de América del Sur durante el Cenozoico: subducción de las placas de Nazca, Farallón y

Aluk: Revista de la Asociación Geológica Argentina, v. 60, p. 797–809.

Sruoga, P., Etcheverría, M.P., Folguera, A., Repol, D., Cortes, J.M., and Zanettini, J.C., 2005, Hoja Geológica 3569-I Volcán Maipo, Provincia de Mendoza: Instituto de Geología y Recursos Minerales, Servicio Geológico Minero Argentino, Boletín 290, 92 p.

Sruoga, P., Rubinstein, N.A., Etcheverria, M.P., Cegarra, M., Kay, S.M., Singer, B., and Lee, J., 2008, Estadio inicial del arco volcánico neógeno en la Cordillera Principal de Mendoza (35°): Revista de la Asociación Geológica Argentina, v. 63, p. 454–469.

Sruoga, P., Rubinstein, N.A., Etcheverria, M., and Cegarra, M., 2009, Volcanismo neógeno y mineralización asociada, Cordillera Principal, Mendoza (35°S): Congreso Geológico Chileno, 12, Actas, CD S11–045, 4 p.

Tassara, A., and Echaurren, A., 2012, Anatomy of the Chilean subduction zone: 3D density model upgraded and compared against global models: Geophysical Journal International, v. 189, p. 161–168, doi:10.1111/j.1365-246X.2012.05397.x.

Tassara, A., Götze, H.-J., Schmidt, S., and Hackney, R., 2006, Three-dimensional density model of the Nazca plate and the Andean continental margin: Journal of Geophysical Research, v. 111, doi:10.1029/2005JB003976.

Tunik, M., Folguera, A., Naipauer, M., Pimentel, M., and Ramos, V.A., 2010, Early uplift and orogenic deformation in the Neuquen basin: Constraints on the Andean uplift from U-Pb and Hf isotopic data of detrital zircons: Tectonophysics, v. 489, p. 258–273, doi:10.1016/j.tecto.2010.04.017.

Turienzo, M.M., 2010, Structural style of the Malargüe fold-and-thrust belt at the Diamante river area (34°30′S–34°50′S) and its linkage with the Cordillera Frontal, Andes of central Argentina: Journal of South American Earth Sciences, v. 29, p. 537–556, doi:10.1016/j.jsames.2009.12.002.

Uliana, M., and Biddle, K., 1988, Mesozoic–Cenozoic paleogeographic and geodynamic evolution of South America: Revista Brasileira de Geociencias, v. 18, p. 172–190.

Uliana, M., Arteaga, M., Legarreta, L., Cerdan, J., and Peroni, G., 1995, Inversion structures and hydrocarbon ocurrence in Argentina, *in* Buchanan, J.G., and Buchanan, P.G., eds., Basin inversion: Geological Society of London Special Publication 88, p. 211–233, doi:10.1144/GSL.SP.1995.088.01.13.

Williams, G.D., Powell, C.M., and Cooper, M.A., 1989, Geometry and kinematics of inversion tectonics, *in* Cooper, M.A., and Williams, G.D., eds., Inversion tectonics: Geological Society of London Special Publication 44, p. 3–15, doi:10.1144/GSL.SP.1989.044.01.02.

Yagupsky, D., Cristallini, E., Fantín, J., Zamora Valcarce, G., Botessi, G., and Varadé, R., 2008, Oblique half-graben inversion of the Mesozoic Neuquén rift in the Malargüe fold and thrust belt, Mendoza, Argentina: New insights from analogue models: Journal of Structural Geology, v. 30, p. 839–853, doi:10.1016/j.jsg.2008.03.007.

Yamada, Y., and McClay, K.R., 2004, 3-D analog modeling of inversion thrust structures, *in* McClay, K.R., ed., Thrust tectonics and hydrocarbon systems: American Association of Petroleum Geologists Memoir 82, p. 276–301.